

On the Interpretation of L- and P-band PolSAR Signatures of Polithermal Glaciers

Giuseppe Parrella^{1,2}, Irena Hajnsek^{1,2}, Kostas Papathanassiou¹

¹German Aerospace Center (DLR) - Microwave and Radar Institute, Wessling (DE)

²ETH Zurich – Department of Environmental Engineering, Zurich (CH)



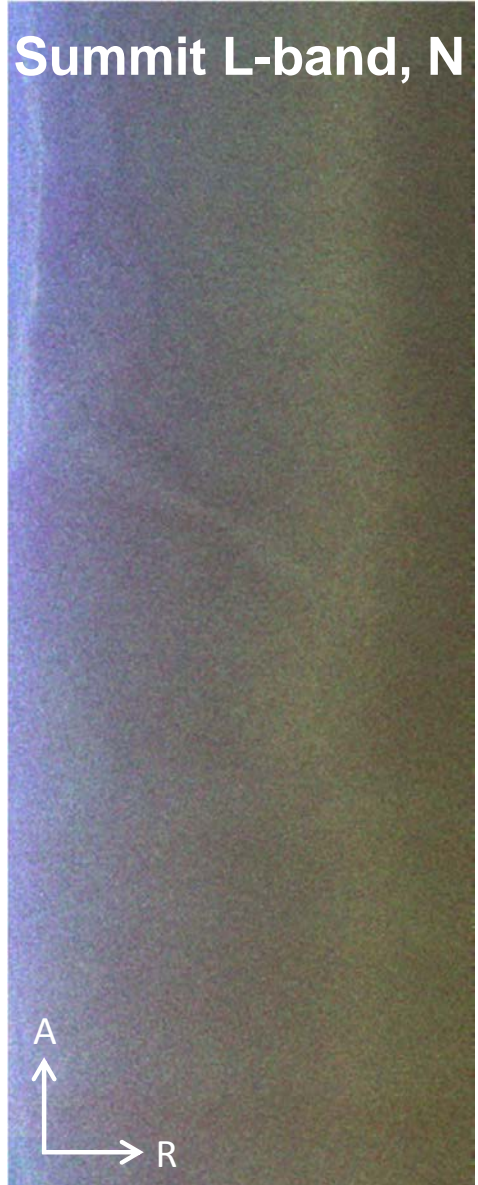
Motivation

- ↗ Interpretation of SAR backscatter to improve **delineation and classification of glacier facies**
- ↗ Quantification of **internal refreezing of melt water** which significantly impacts mass balance
- ↗ Understanding and quantification of **glacier dynamics** occurring as consequence of climate changes
- ↗ Derive **penetration depth** to be used for correcting penetration bias in InSAR and radar altimeter products
- ↗ Long wavelength, in this case **L- and P-band**, SARs penetrate up to some tens of meters into the ice
 - ↗ Suitable to investigate **subsurface structure** of glacier facies

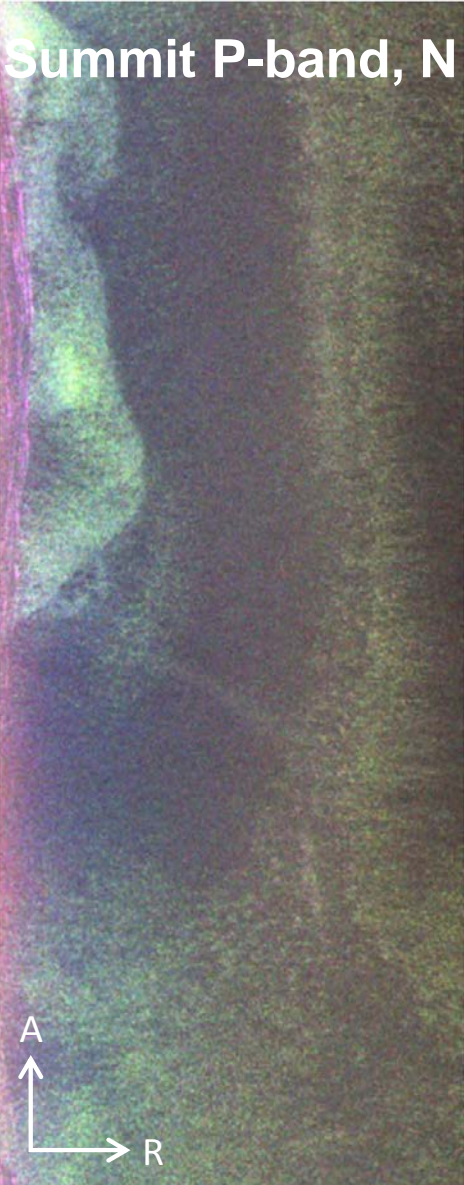
Test Site: Nordaustlandet, Svalbard

- **Etonbreen and Summit of the Austfonna ice cap, Svalbard Archipelago, Norway ($\sim 80^\circ\text{N}$, 24°E)**

Summit L-band, N

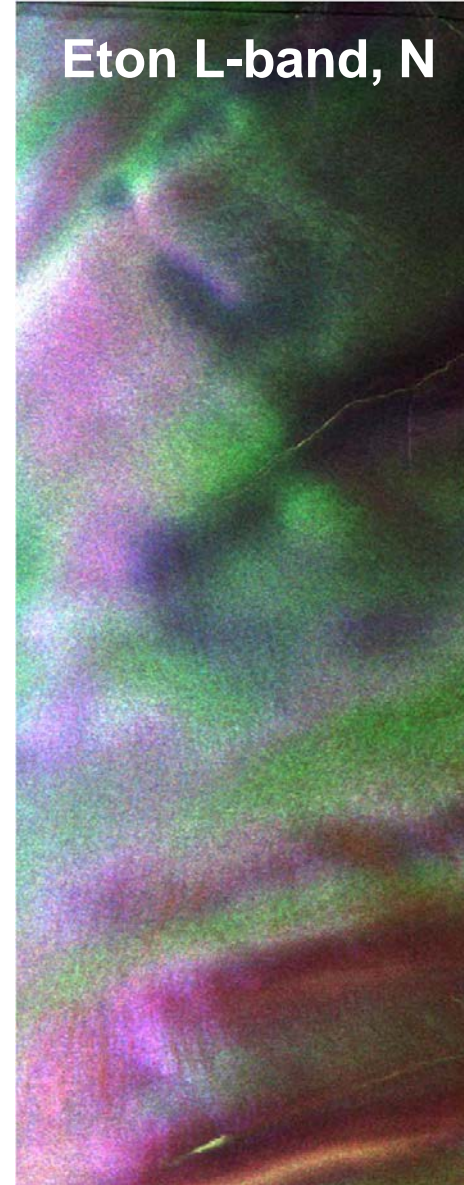


Summit P-band, N



↑
10 Km

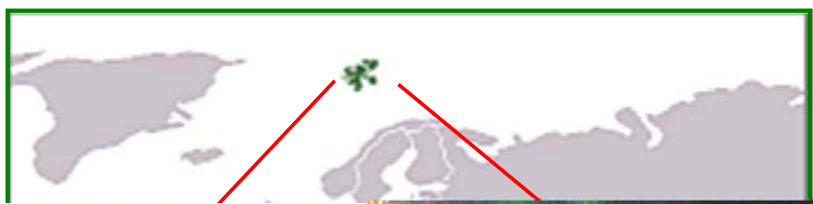
Eton L-band, N



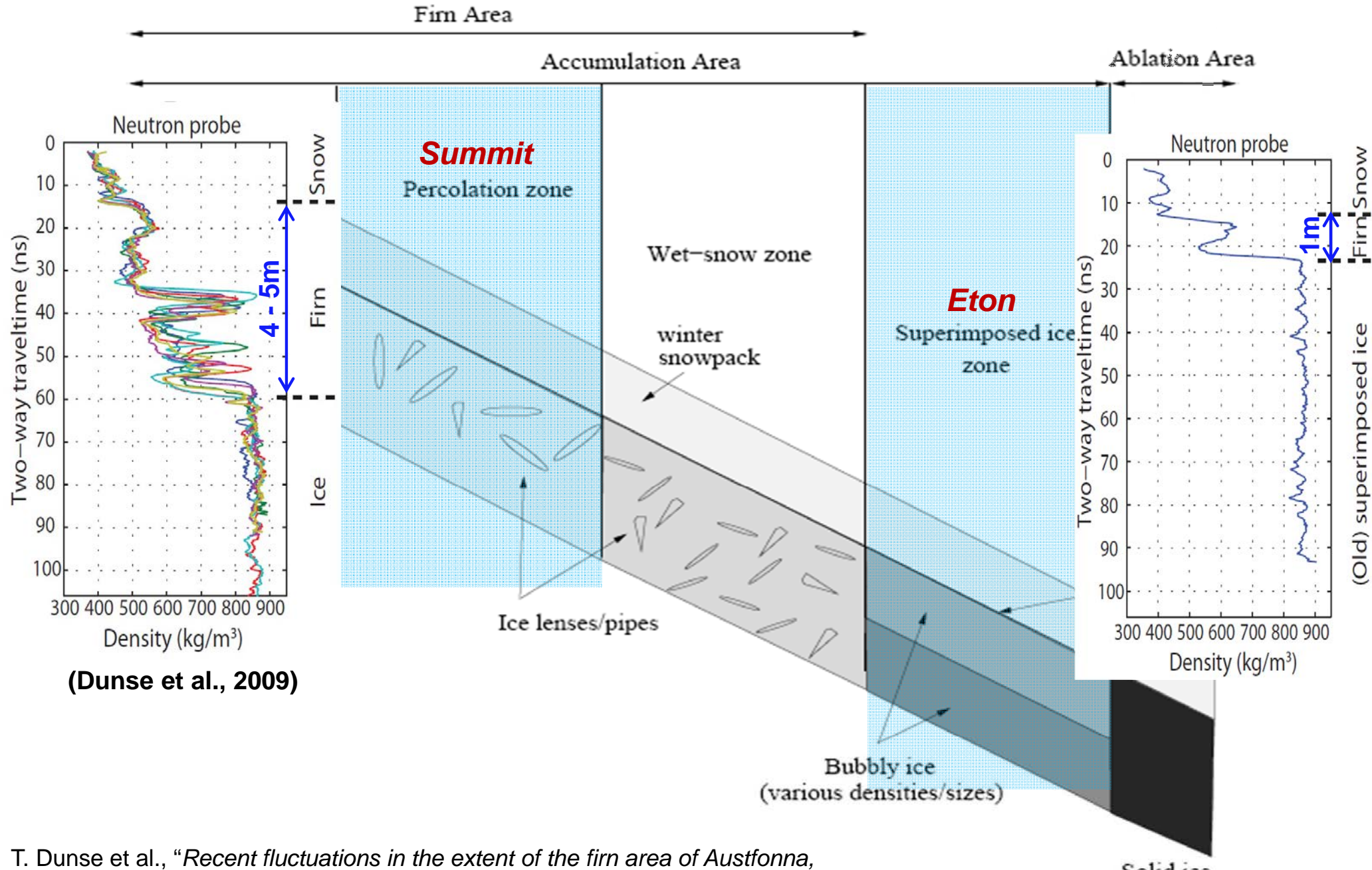
Eton P-band, N



3 Km



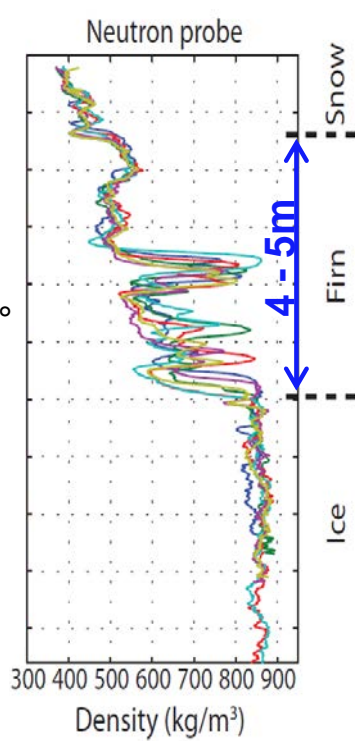
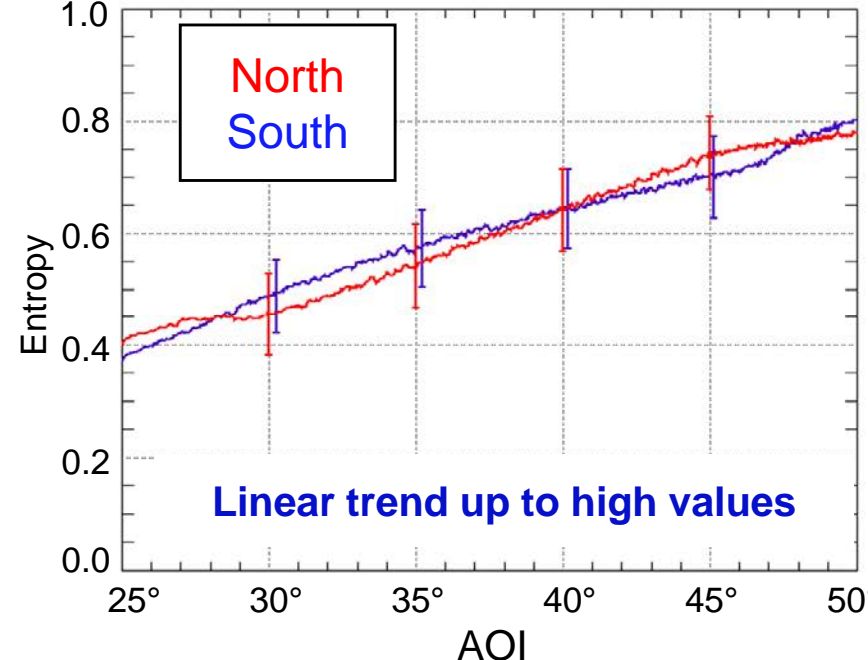
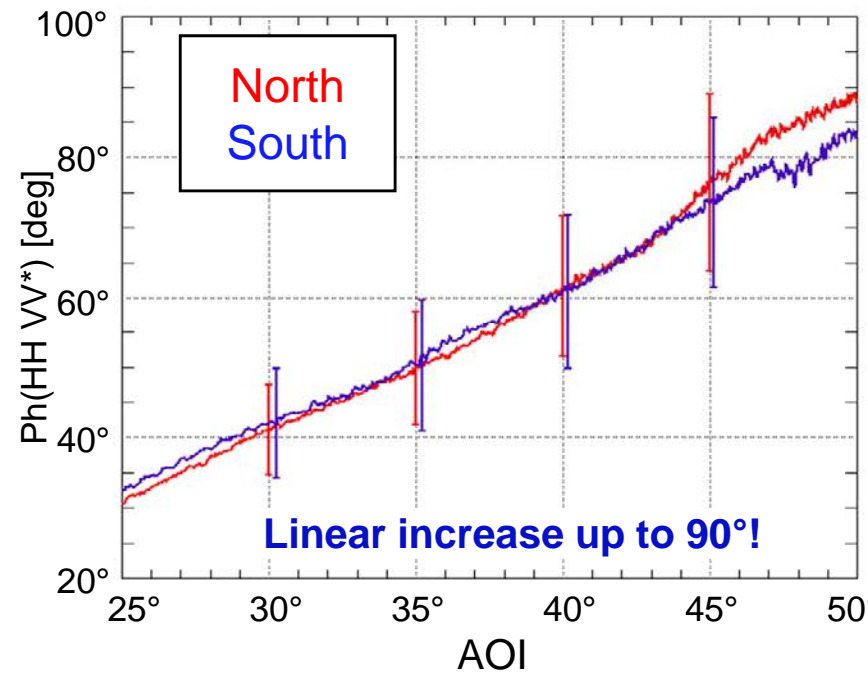
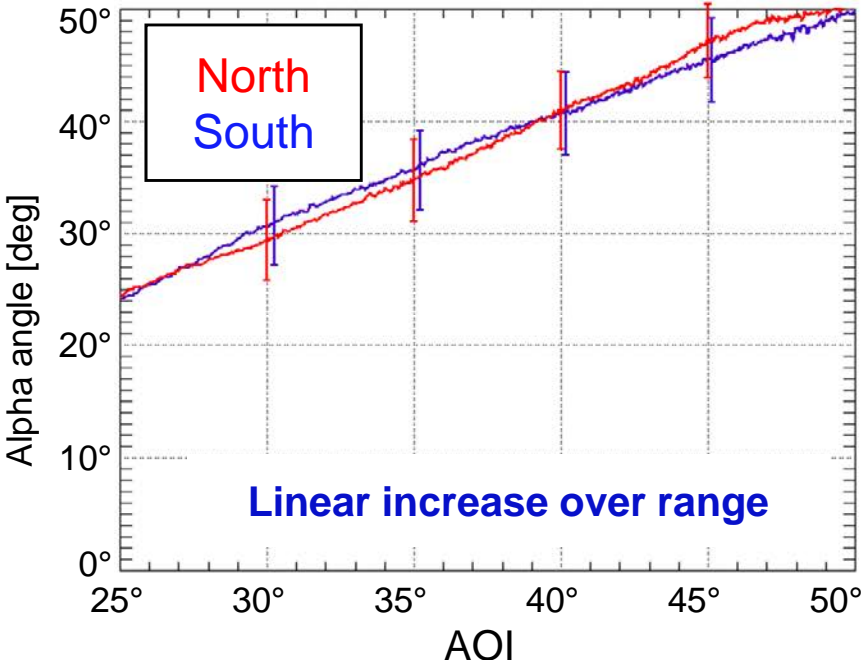
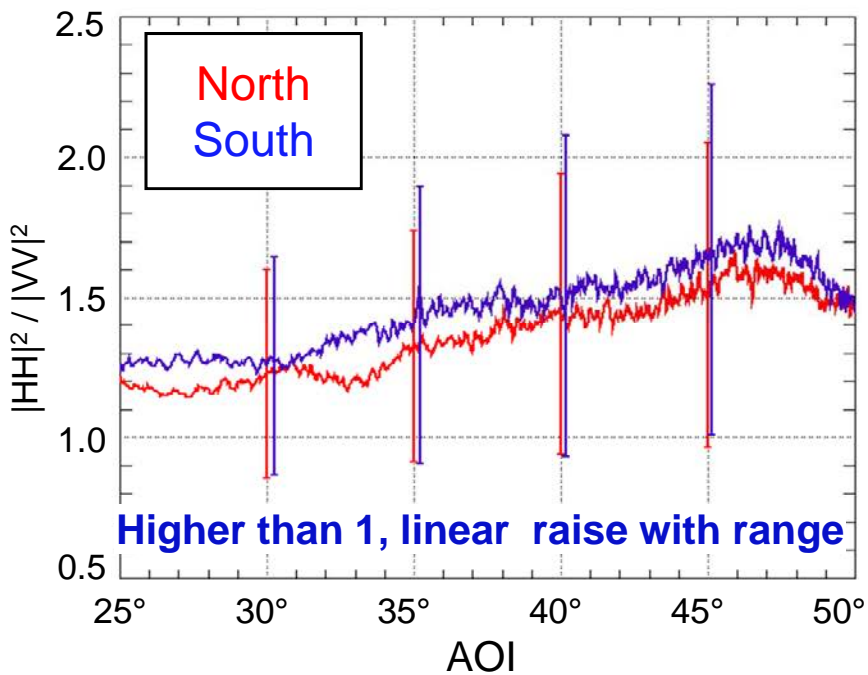
Glacier Facies



T. Dunse et al., "Recent fluctuations in the extent of the firn area of Austfonna, Svalbard, inferred from GPR", *Annals of Glaciology*, vol .50, pp. 155-162, 2009.

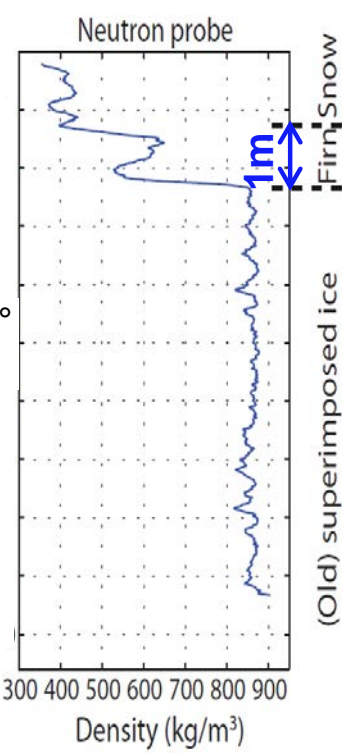
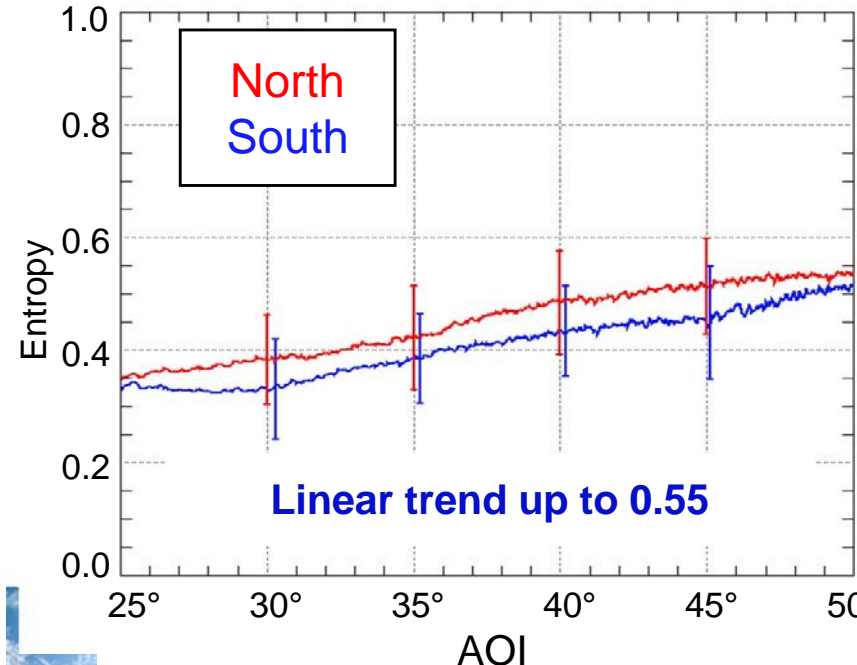
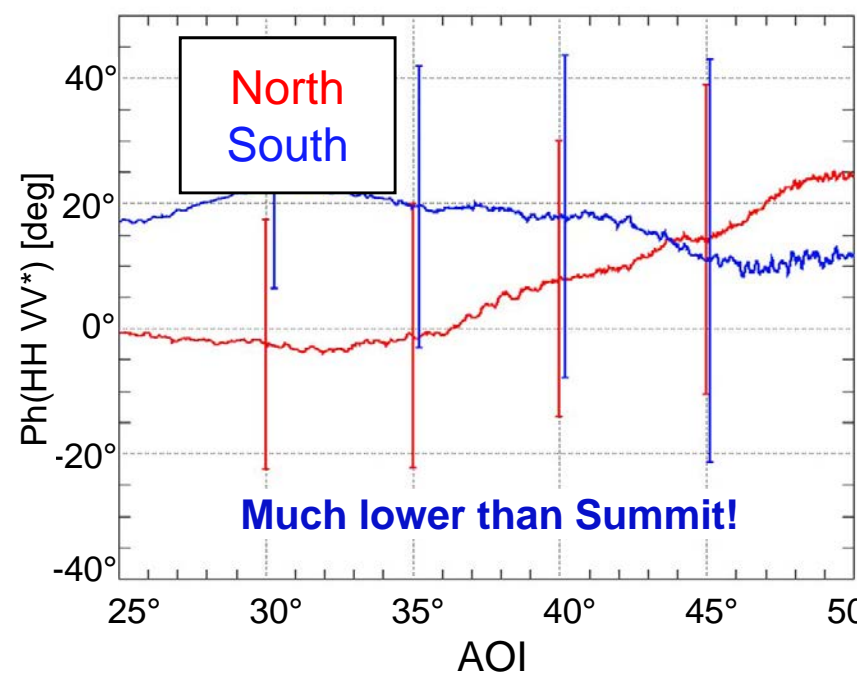
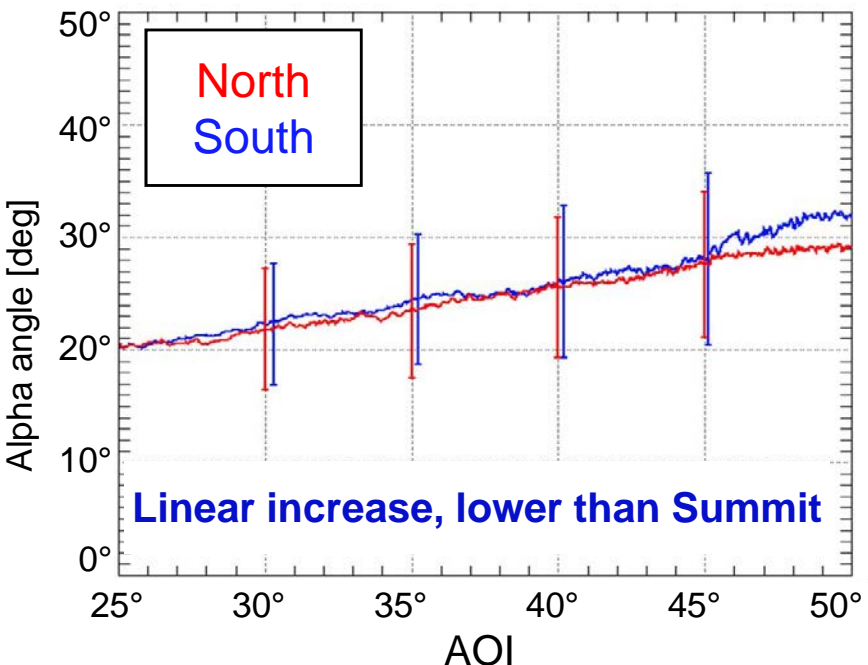
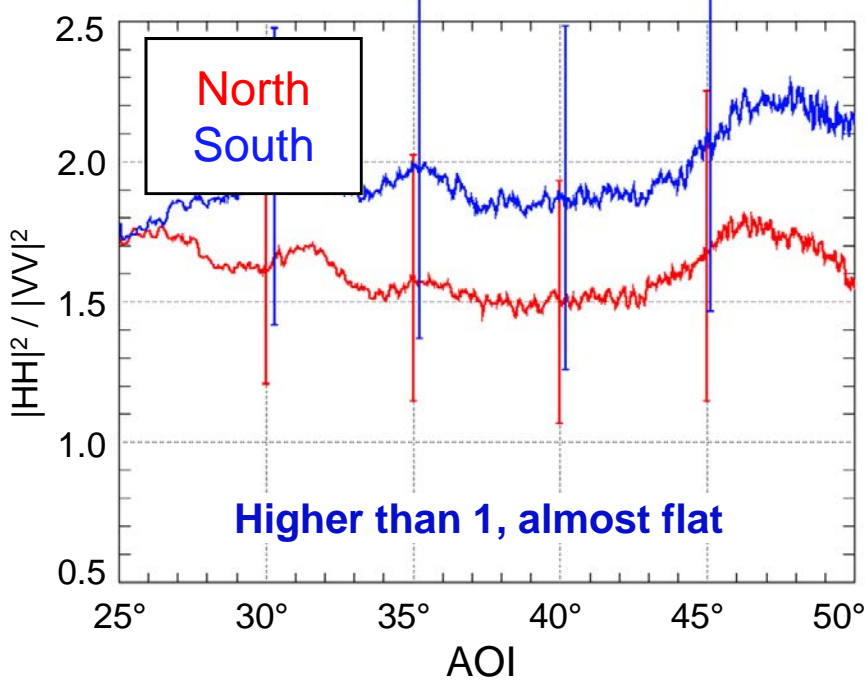
L-band Polarimetric Signatures - Summit

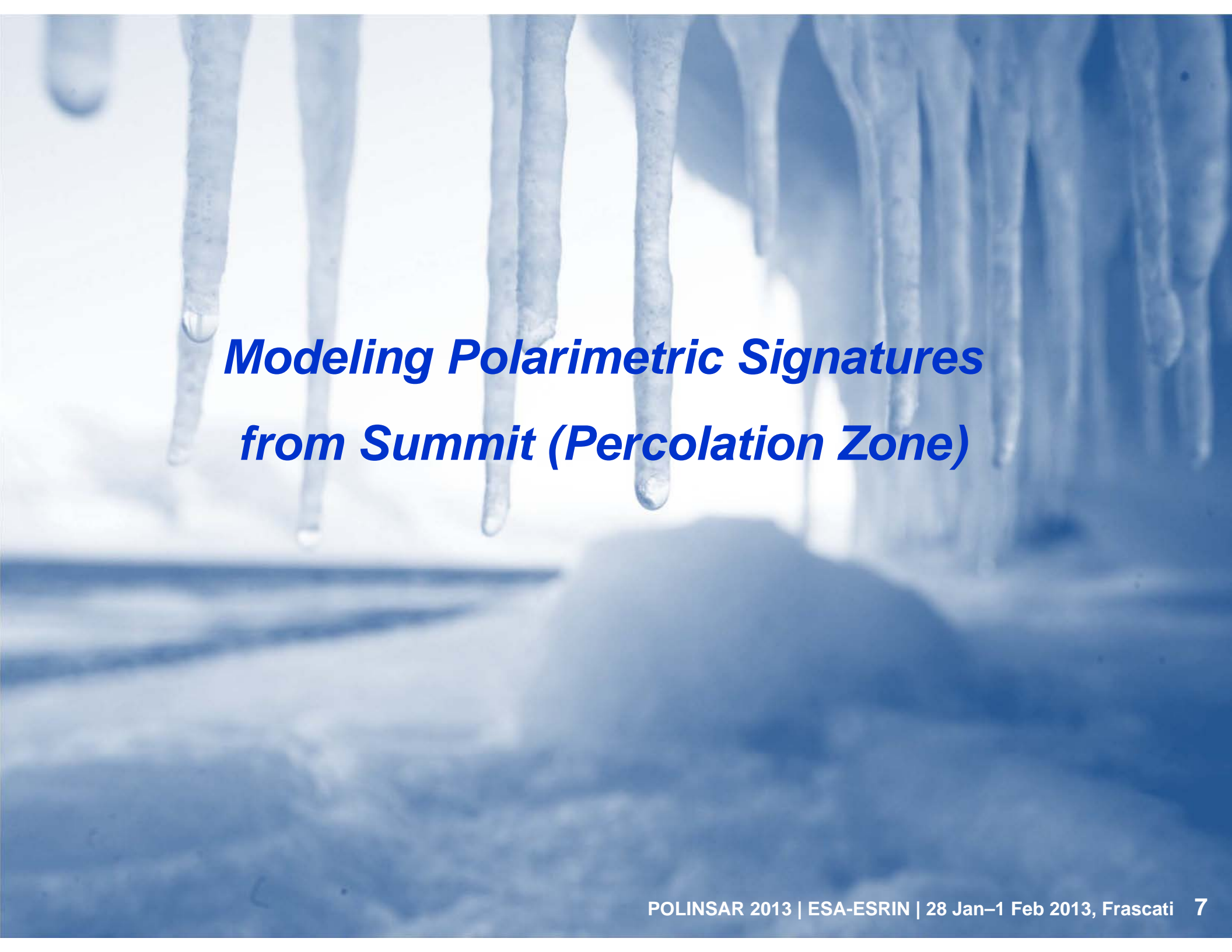
↗ Average along azimuth direction



L-band Polarimetric Signatures - Eton

↗ Average along azimuth direction



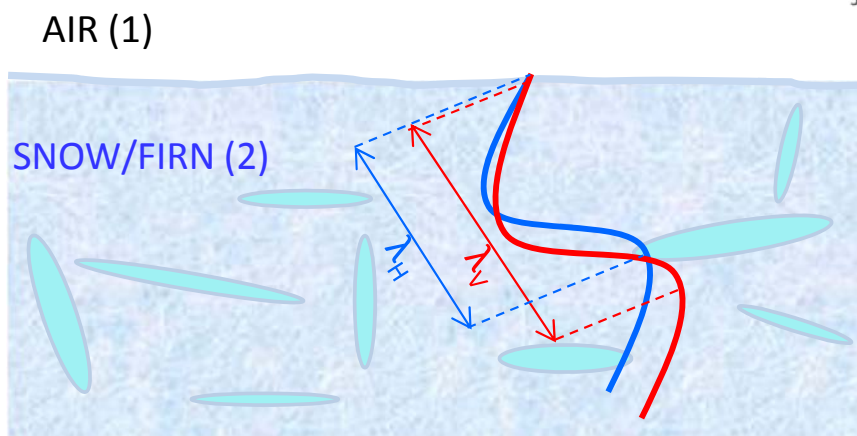
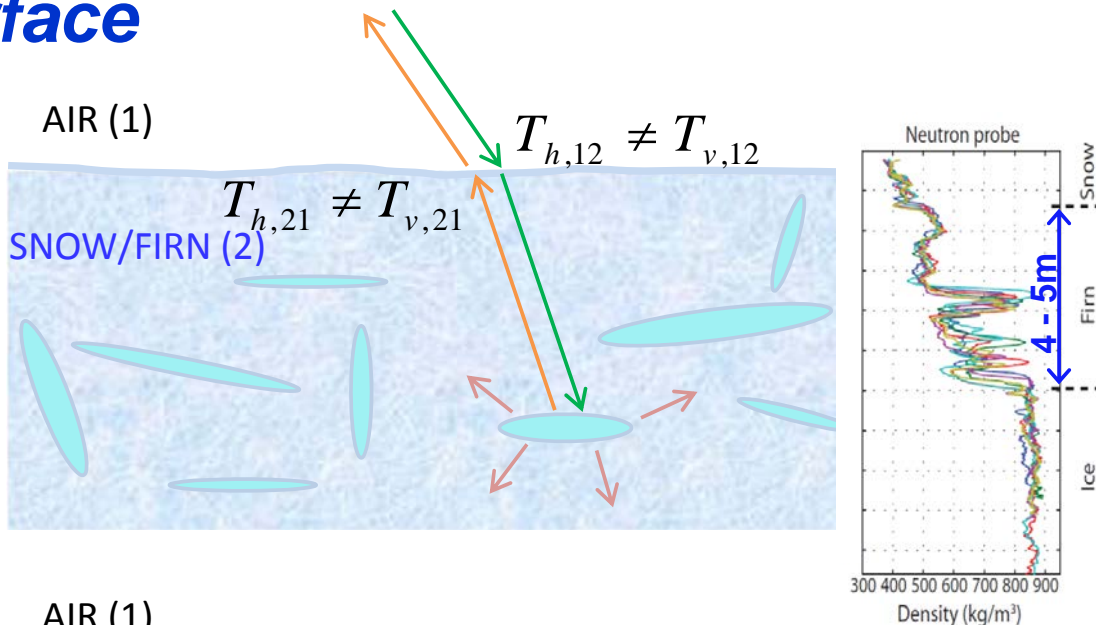


Modeling Polarimetric Signatures from Summit (Percolation Zone)

Modeling the Glacier Subsurface

Scattering from Percolation Zone

- ↗ Particle Scattering Model (*Cloude et al., 1999*) for ice pipes and lenses in firn
 - ↗ Inclusion of **incidence angle** dependency
 - ↗ **Transmission effects** at glacier surface (air/snow interface)
 - ↗ **Differential propagation** effects (*Cloude et al., 2000*) due to dielectric anisotropy of polar firn ($n_{hh} \neq n_{vv}$) i.e. differential propagation phase and losses



$$[C_{tot}] = f_{lenses} \cdot [T][P][C_{lenses}][T]^t[P]^t + f_{pipes} \cdot [T][P][C_{pipes}][T]^t[P]^t + [N]$$


 Transmission Propagation effects

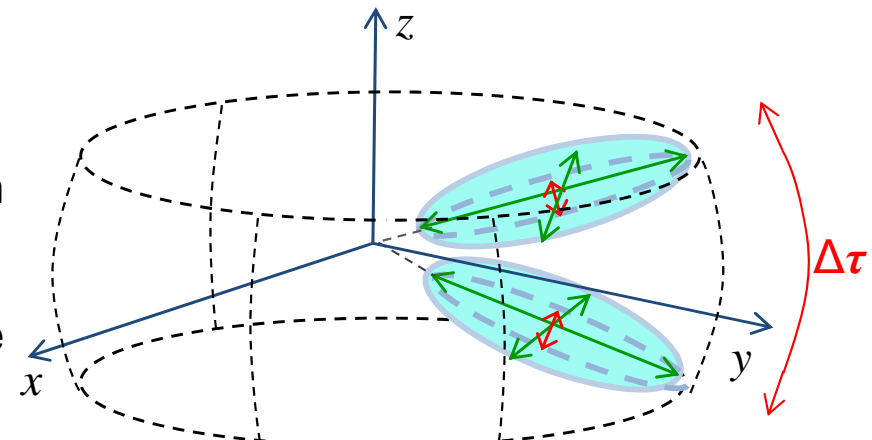
S.R. Cloude et al., "Wide-band Polarimetric Radar Inversion Studies for Vegetation Layers", IEEE TGRS, vol. 37, n. 5, Sept. 1999.

S.R. Cloude et al., "The Remote Sensing of Oriented Volume Scattering Using Polarimetric Radar Interferometry", Proc. of ISAP2000, Fukuoka, Japan.

Modeling the Glacier Subsurface

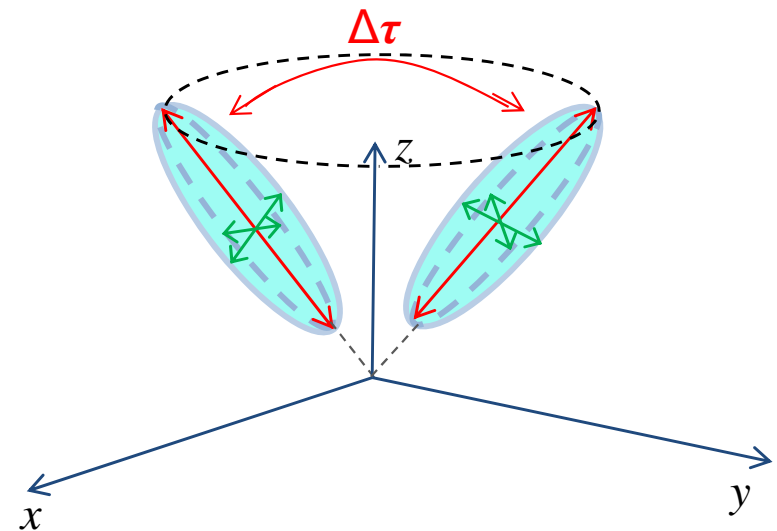
Ice Lenses

- ↗ Extent up to some tens of cm, few mm to some cm thick (Jezek et al., 1994)
- ↗ Typically oriented parallel to the firn surface (plane x-y)
- ↗ Modelled as (mainly) **horizontal oblates** ($A_p \ll 1$)



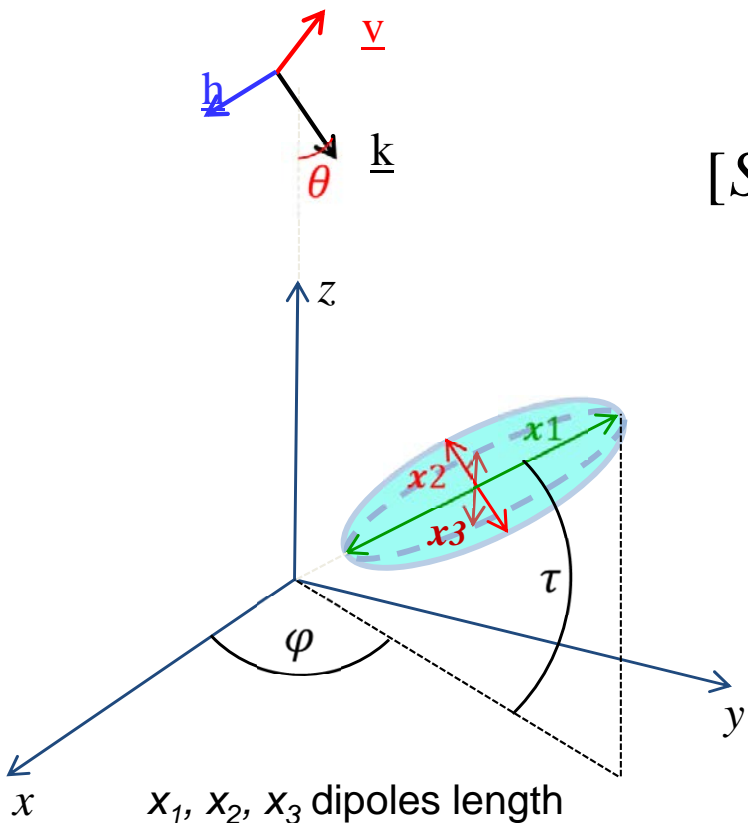
Ice Pipes

- ↗ Length up to some tens of cm , thickness of few cm
- ↗ Mainly vertically oriented (Jezek et al., 1994)
- ↗ Modelled as **vertical prolates** ($A_p > 1$)



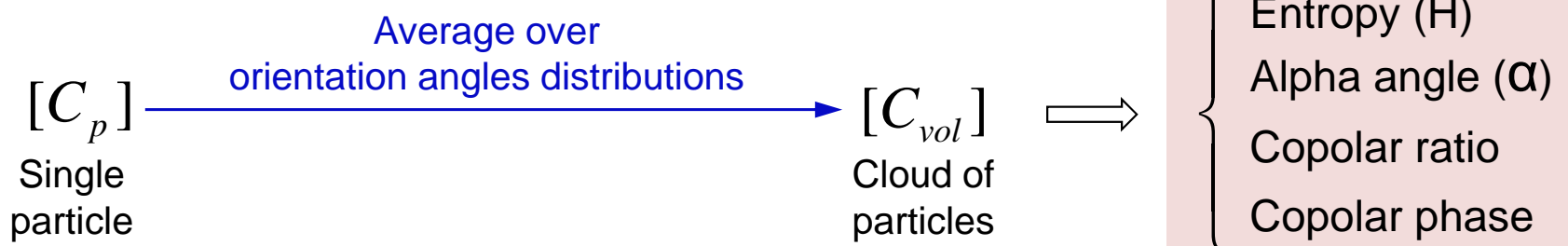
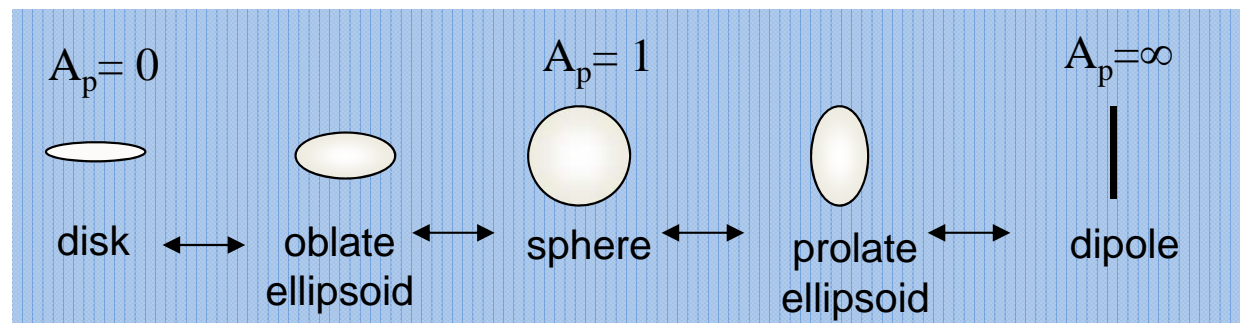
K.C. Jezek, S.P. Gogineni, M Shanbleh, "Radar Measurements of melt zones on the Greenland Ice Sheet", Geophys. Res. Letters, vol. 21, pp. 33-36, 1994.

Particles Scattering Model



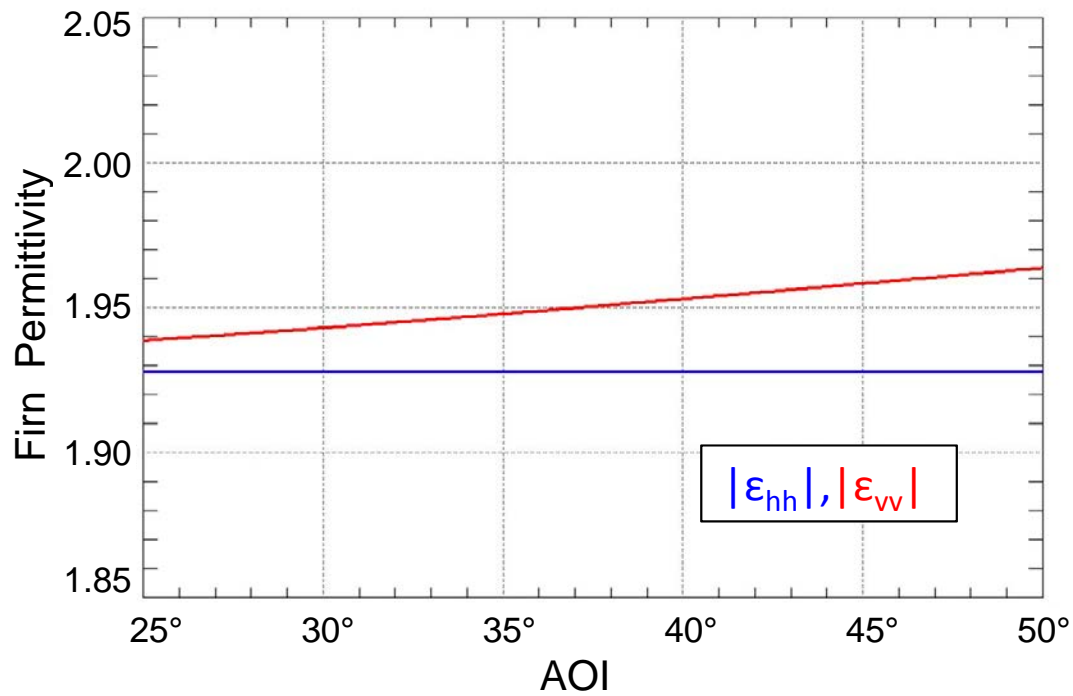
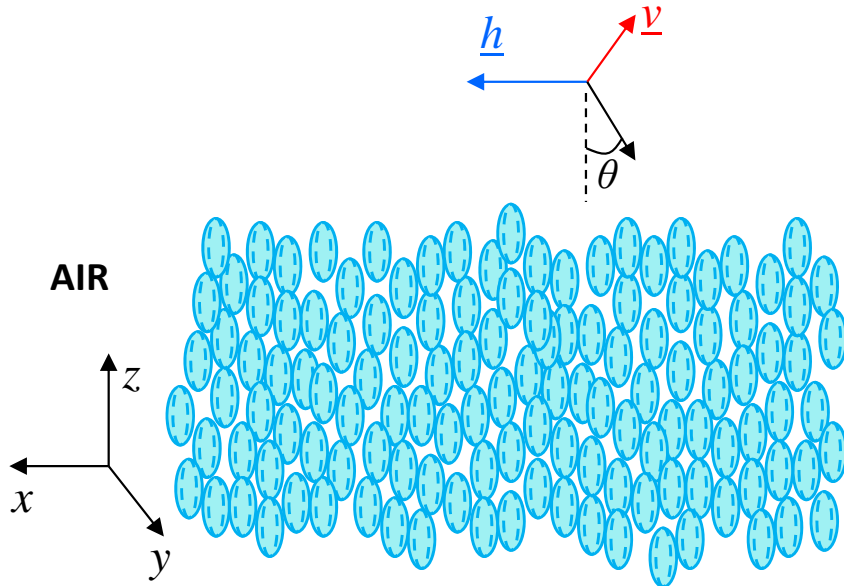
$$[S_p(A_p, \vartheta, \phi, \tau)] = \begin{bmatrix} S_{hh}(A_p, \vartheta, \phi, \tau) & S_{hv}(A_p, \vartheta, \phi, \tau) \\ S_{vh}(A_p, \vartheta, \phi, \tau) & S_{vv}(A_p, \vartheta, \phi, \tau) \end{bmatrix}$$

$A_p = f(x_1, x_2, x_3)$ particle shape factor



Differential Propagation Effects

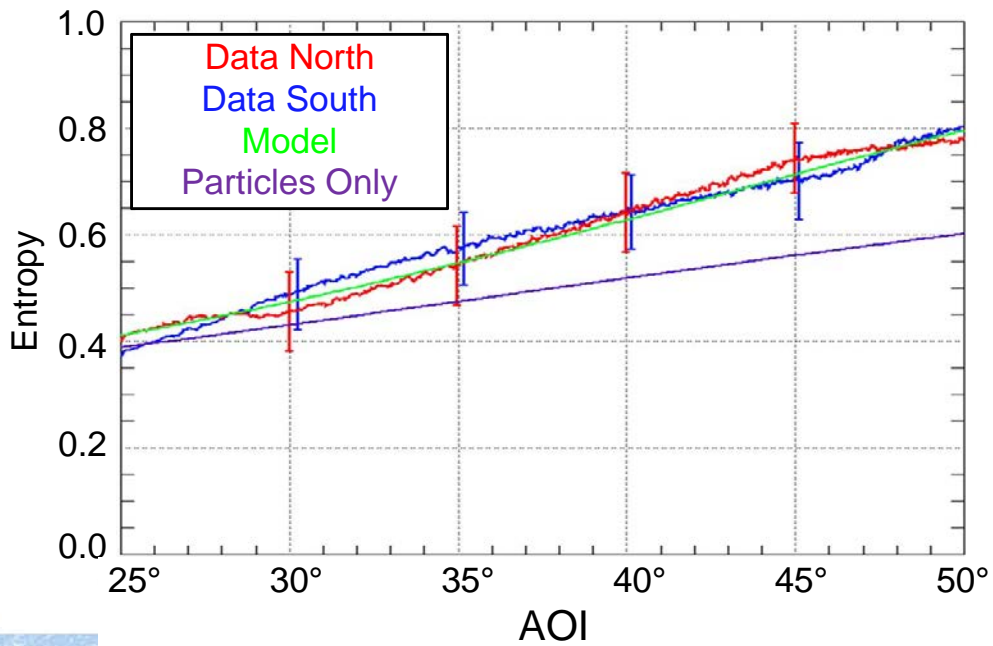
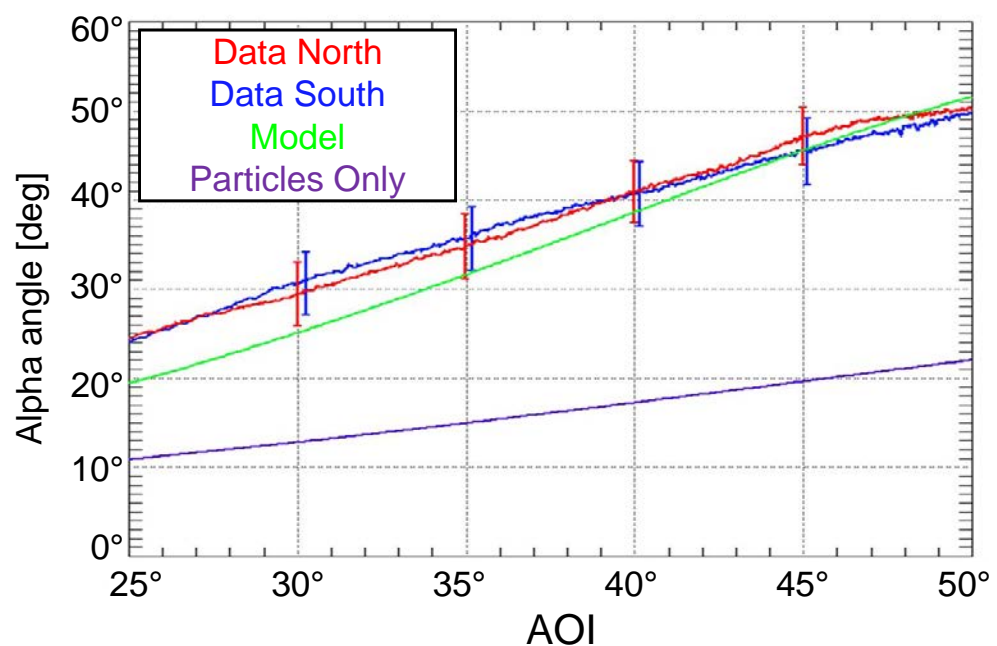
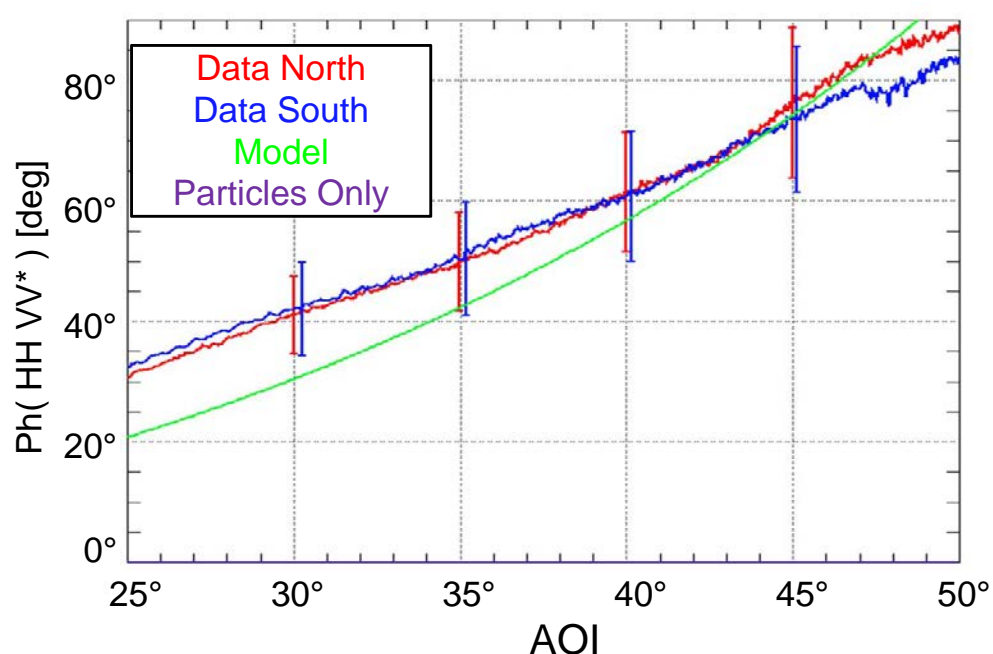
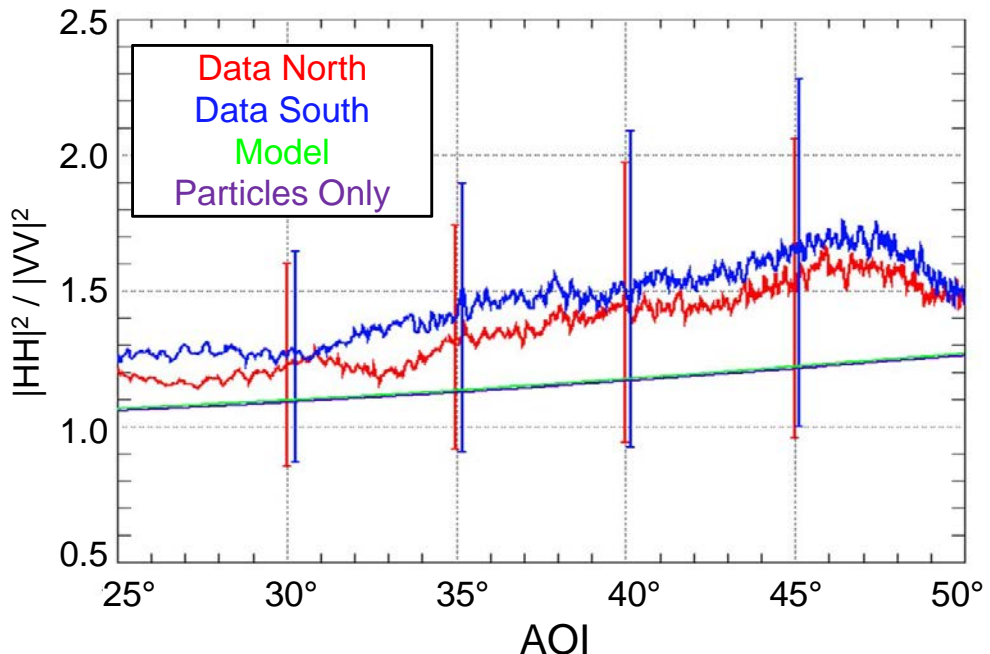
- Polar Firn is an **anisotropic medium** (Alley 1987)
 - Vertically oriented grains in air background
 - Prolate spheroidal shape (axis ratio ~1.2-1.4)
 - Size of few mm
 - Density of 0.4-0.7 Kg/m³
- **Effective permittivity** for a two-phase mixture (Sihvola et al., 1988)
 - Ice grains in air background
 - 60-70% volume fraction of grains
 - Prolate spheroids with $Ap = 1.3$



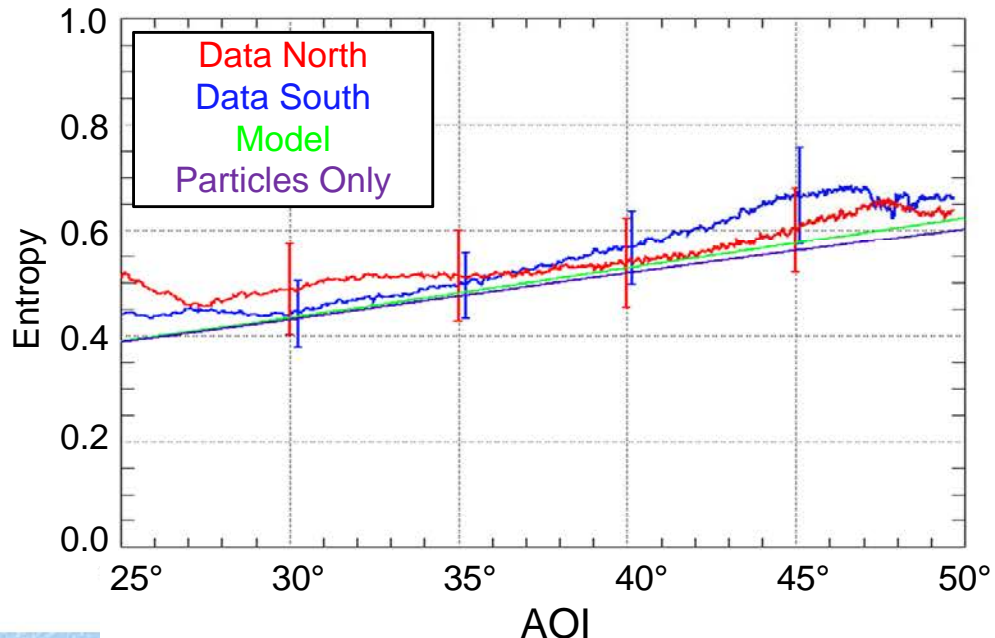
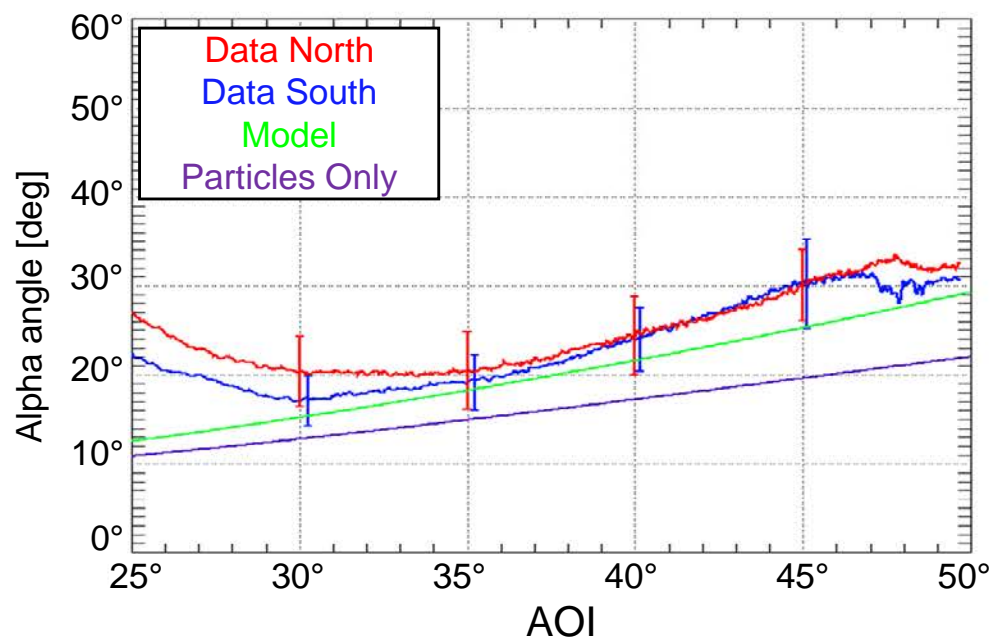
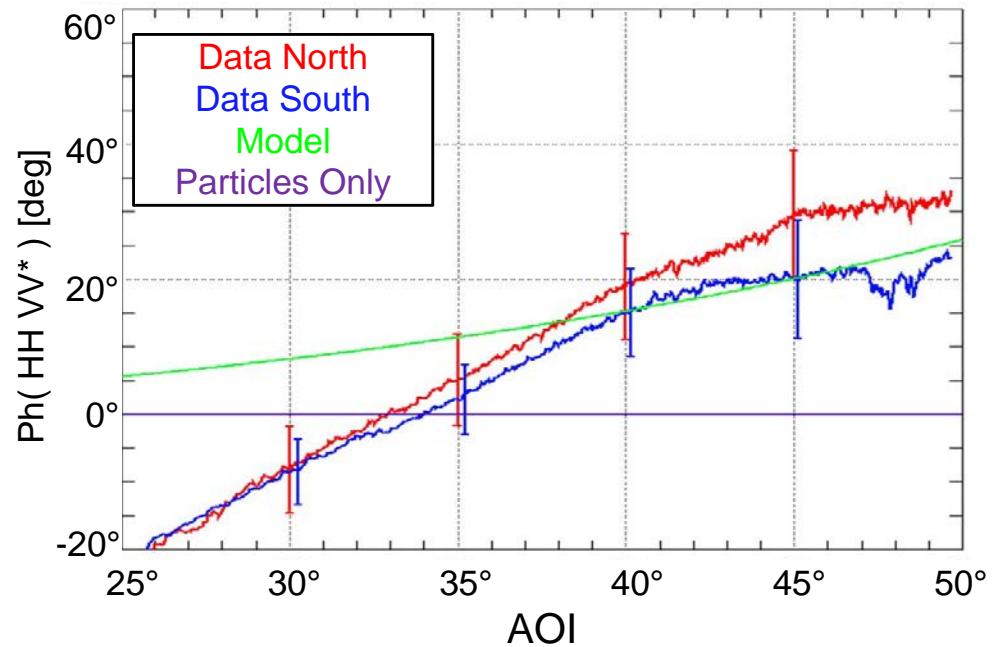
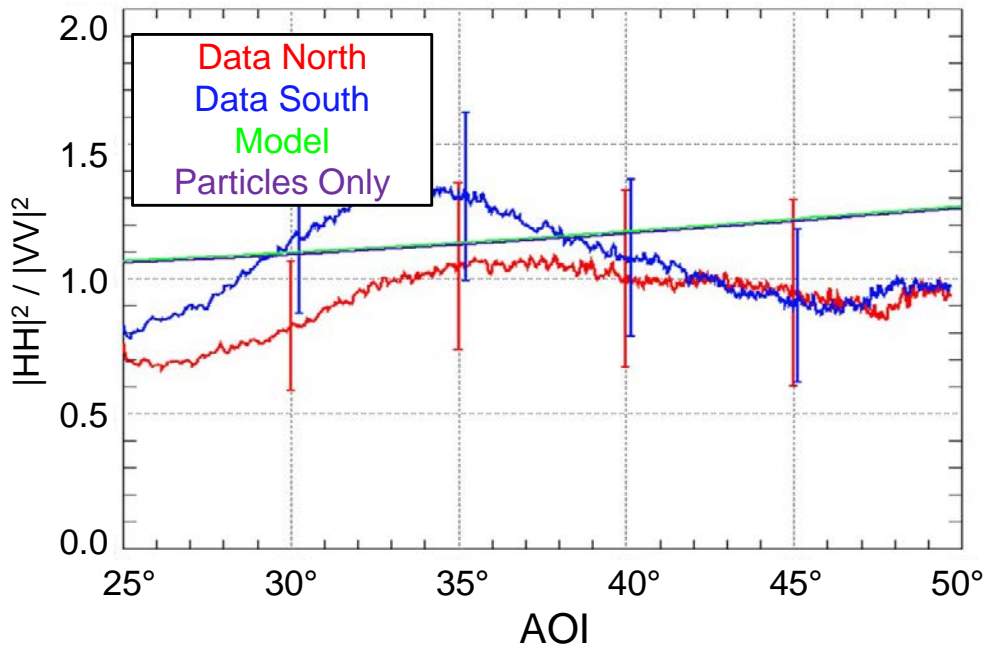
R.B. Alley, "Texture of Polar Firn for Remote Sensing", Annals of Glaciology, vol. 9, 1987

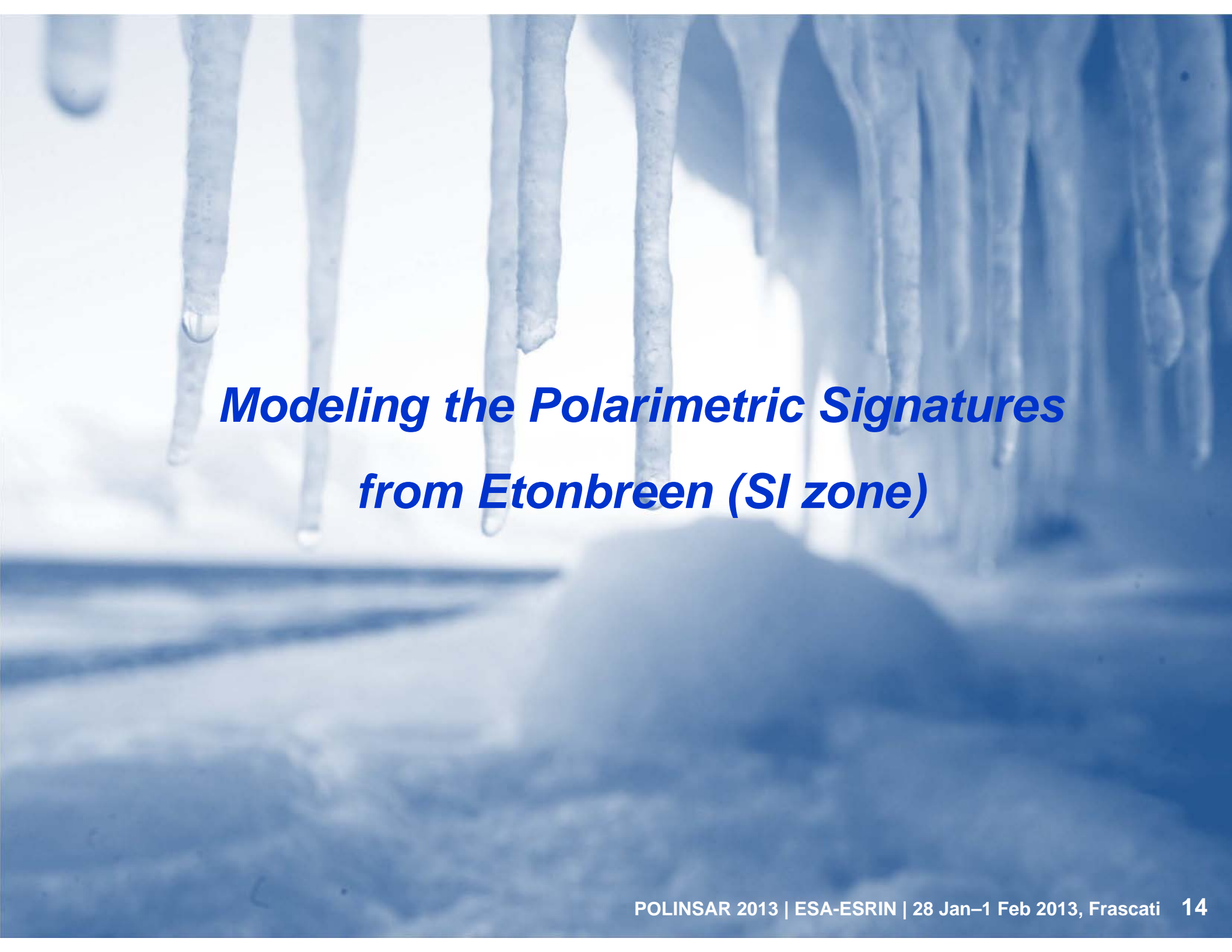
A. Sihvola and Jin Au Kong, "Effective Permittivity of Dielectric Mixtures", IEEE TGRS, vol. 9, n. 4, 1988

Model vs L-band Data, Summit



Model vs P-band Data, Summit



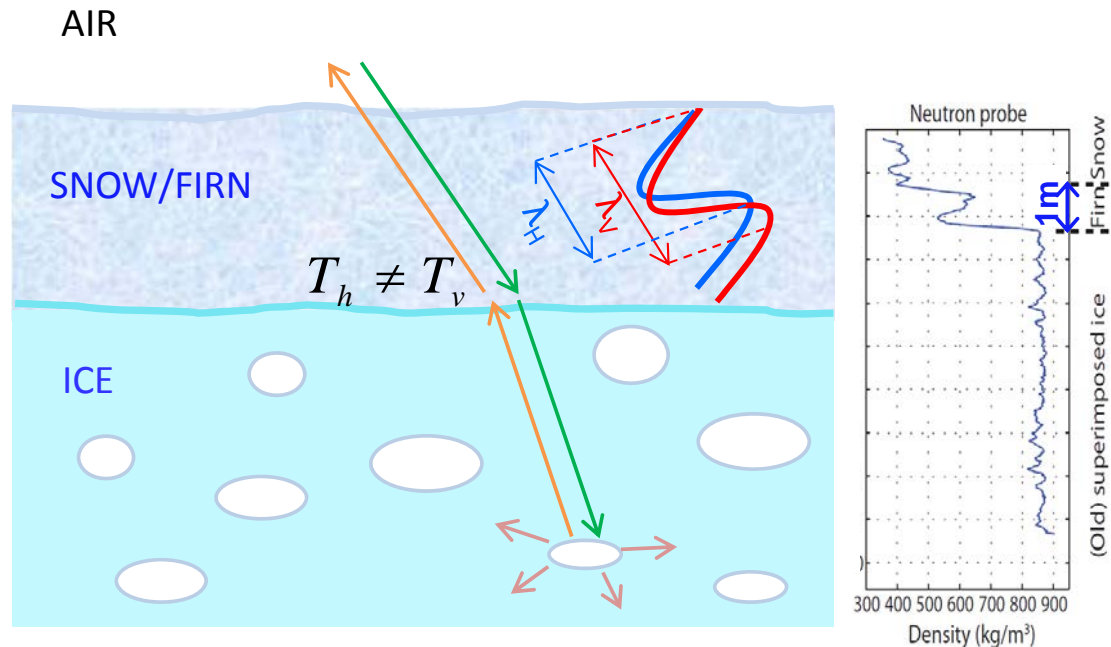


Modeling the Polarimetric Signatures from Etonbreen (SI zone)

Modeling the Glacier Subsurface

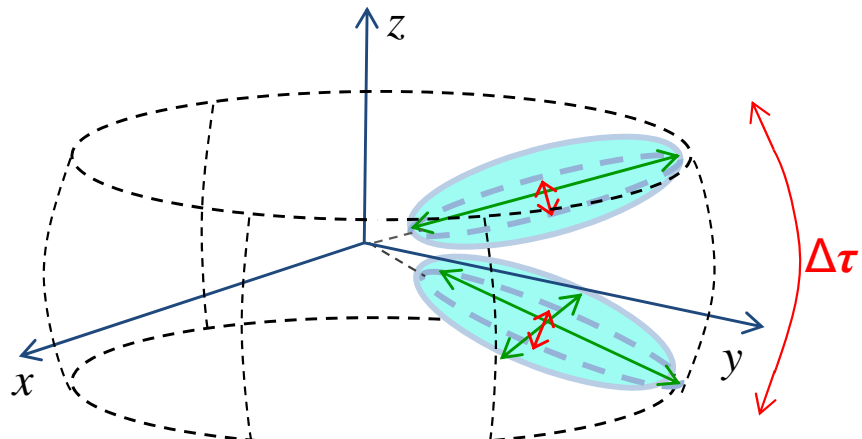
Scattering from SI Zone

- Particle Scattering Model (*Claude et al., 1999*) for bubbly ice (air bubbles)
- Overlying snow/firn layer (1-2m) from previous winter

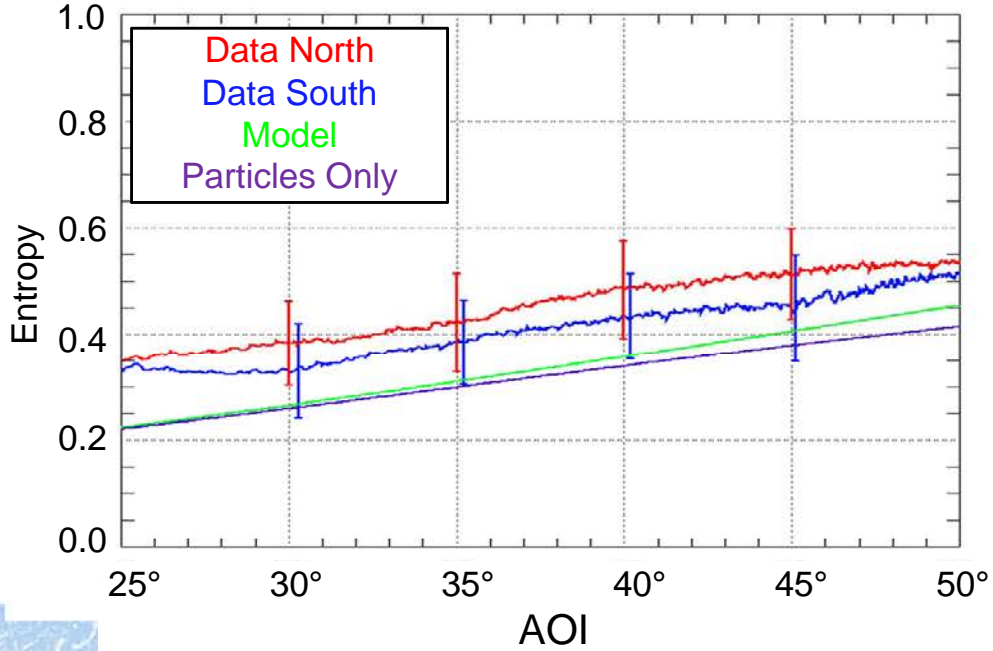
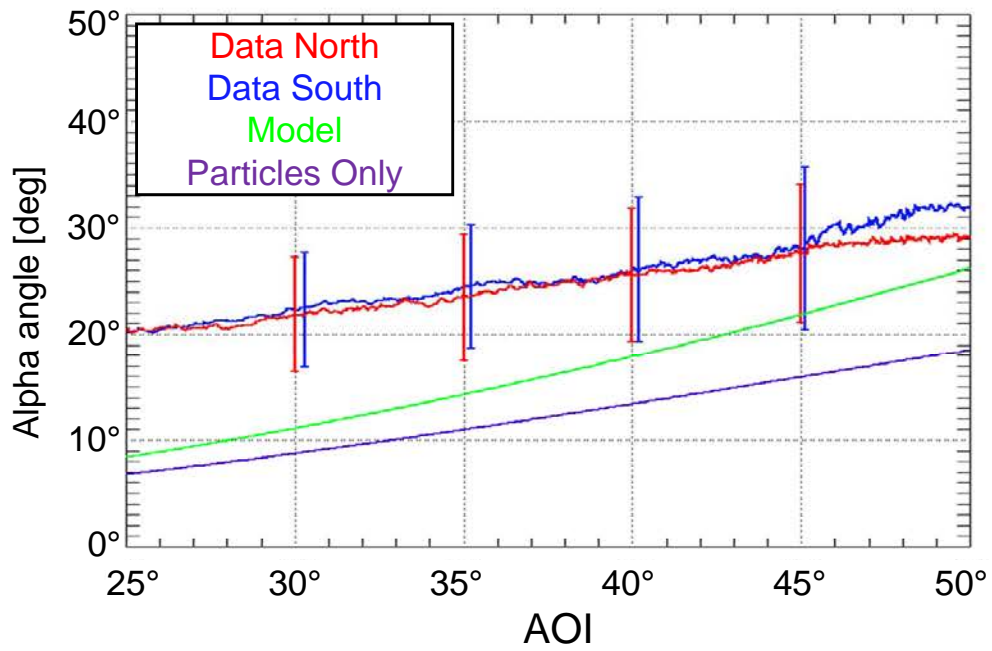
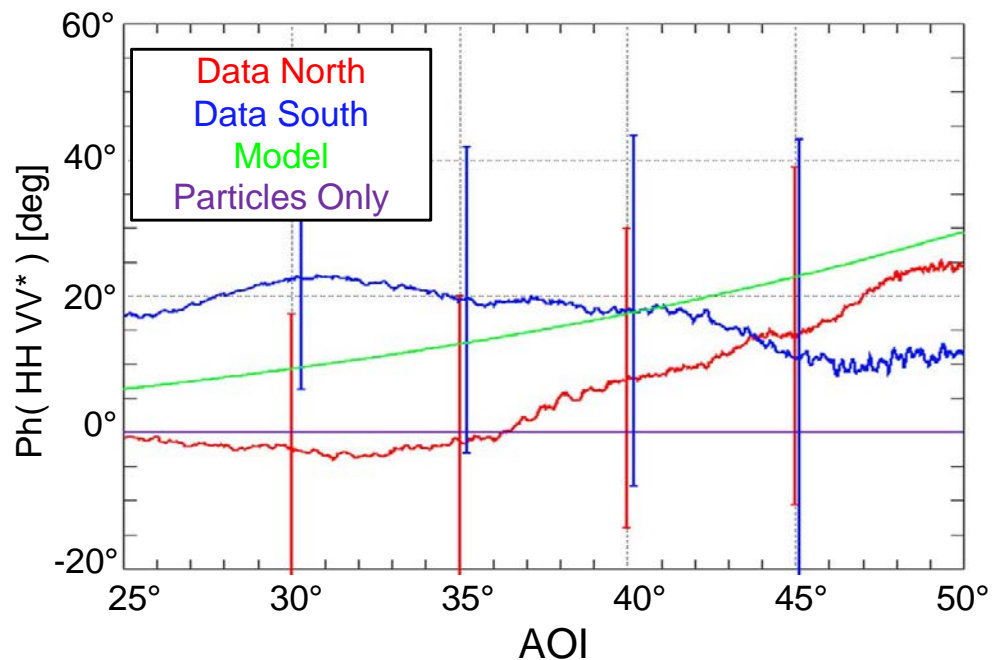
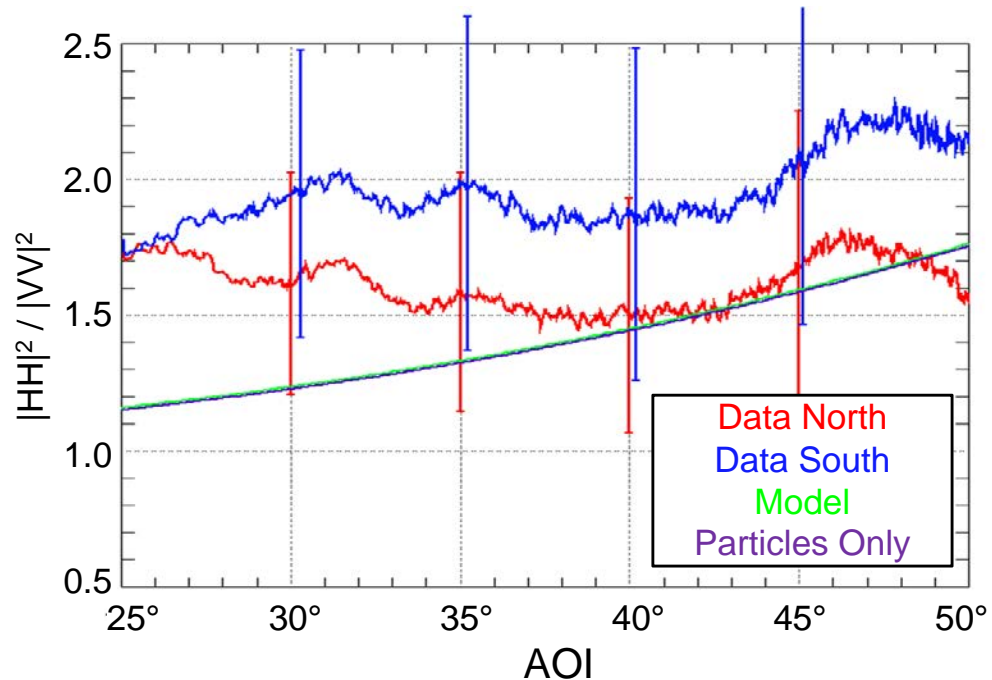


Air Bubbles

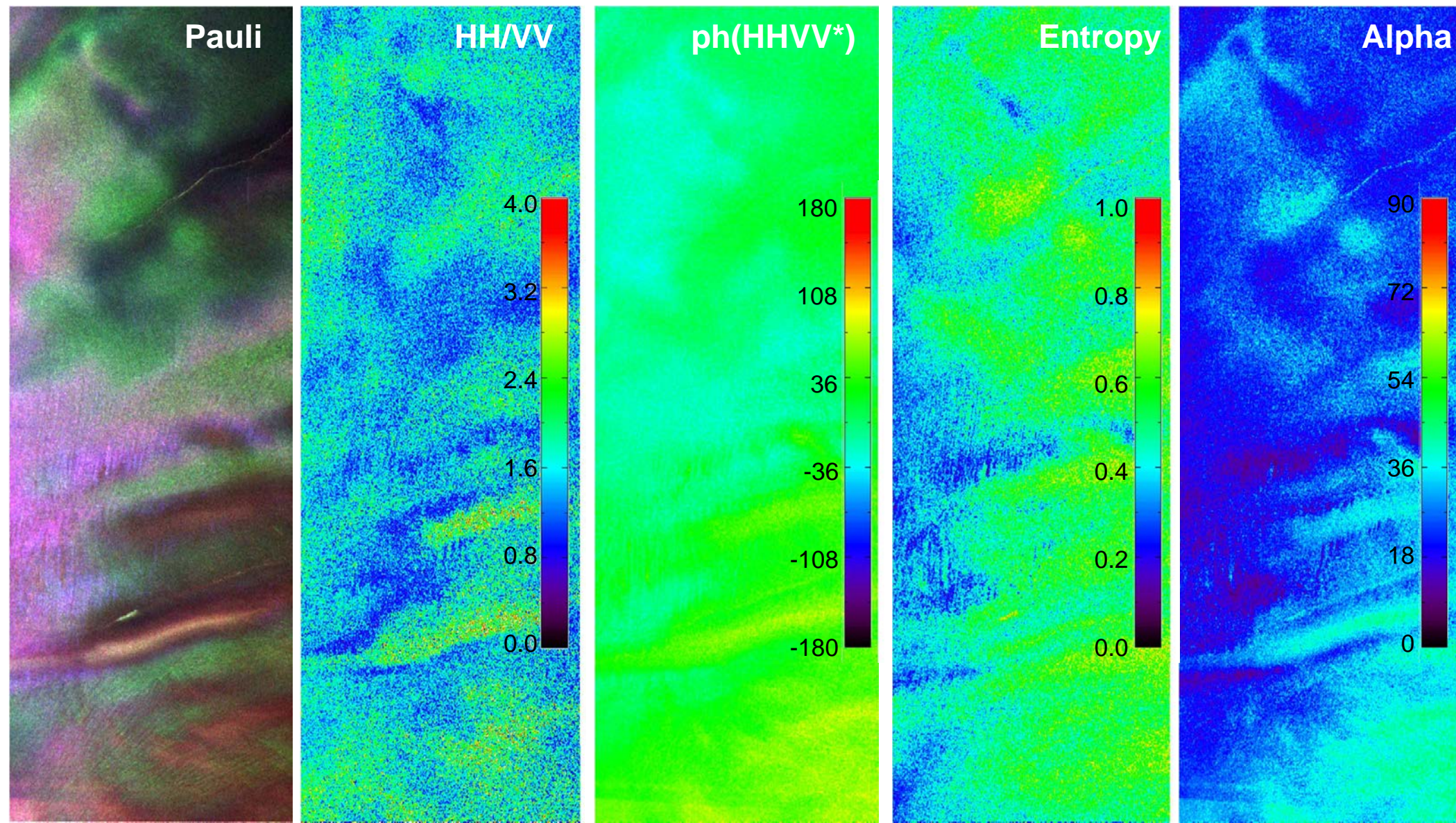
- Volume fraction depend on ice formation conditions
- Typical size are 1mm to 1cm
- Can have elongated shape due to pressure or temperature
- Modelled as (mainly) horizontal oblates ($Ap < 1$)



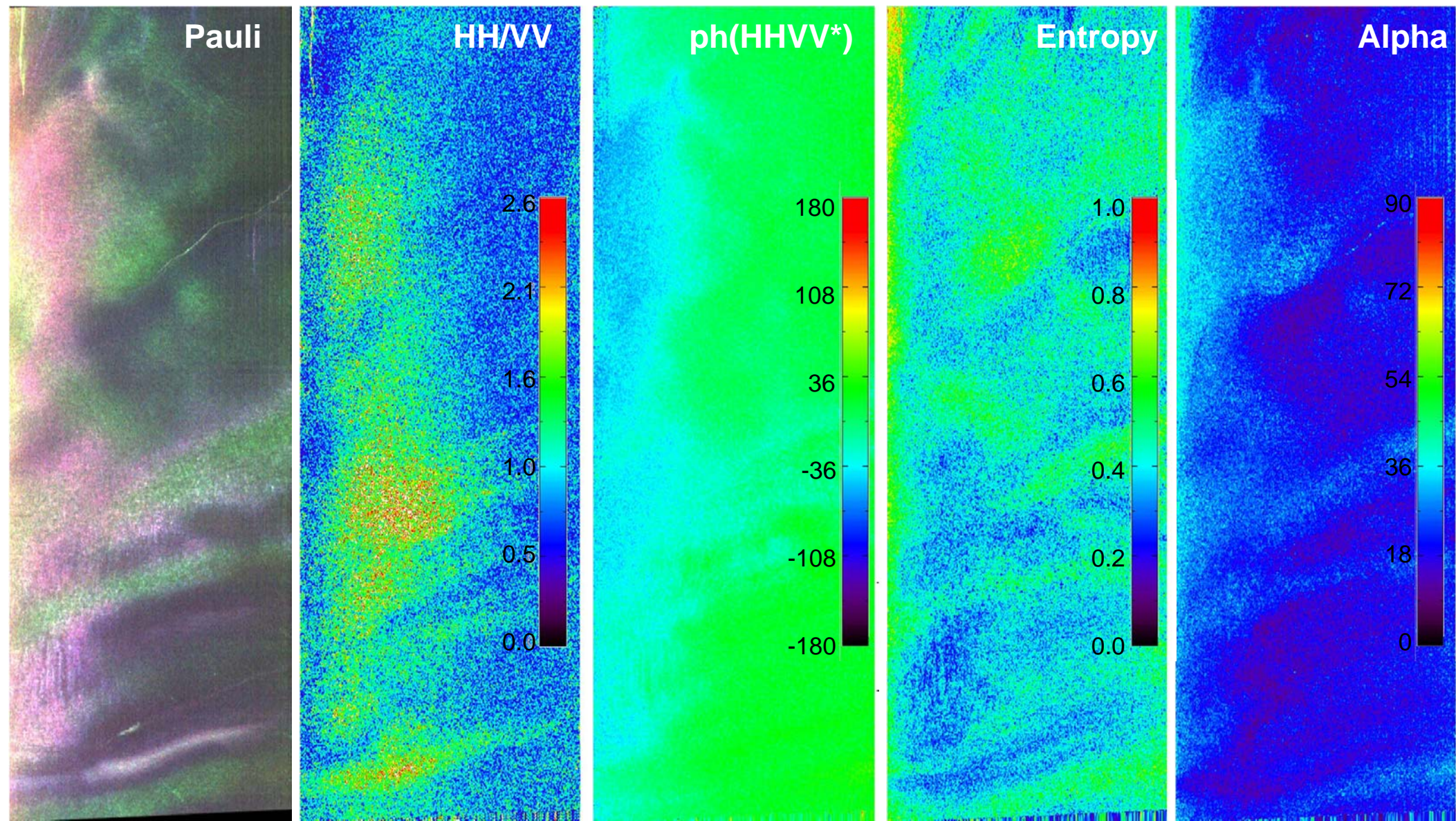
Model vs L-band Data, Eton



PolSAR Signatures Eton, L-band



PolSAR Signatures Eton, P-band



Conclusions

- ↗ Modeling of backscatter contributions from subpolar glaciers
 - ↗ Adaptation of **Particle Scattering Model** for different glacier facies
- ↗ Inclusion of **incidence angle** to explain geometry dependency of polarimetric signatures
- ↗ **Particle shape** can explain **co-polar ratio** observed in the data
- ↗ **Firn anisotropy** might explain **co-polar phase** difference, **H** and **α**
 - ↗ Modeling of **differential propagation** effects
- ↗ **Percolation zone**
 - ↗ Particle Scattering Model for ice **pipes** and **lenses** (prolate/oblate spheroids) in firn background
 - ↗ Model prediction matches quite well the **L-band** data
 - ↗ **P-band** data reveals possible buried local structures → Not included in the modeling
- ↗ **Superimposed Ice zone**
 - ↗ Particle Scattering Model for **bubbly ice**
 - ↗ SI formation depends on local topography → Very irregular PolSAR signatures

Next Steps

- ↗ Further modeling for SI zone → Account for heterogeneity of the test site
 - ↗ Possible internal interactions between layers with different bubble content

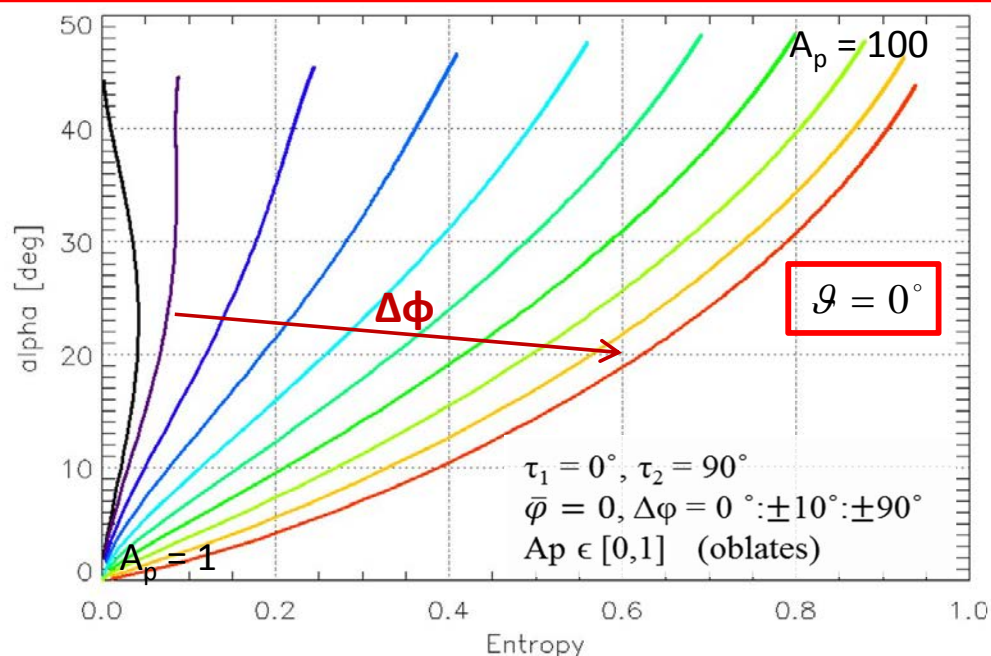
Thanks for your attention!

... Questions ?

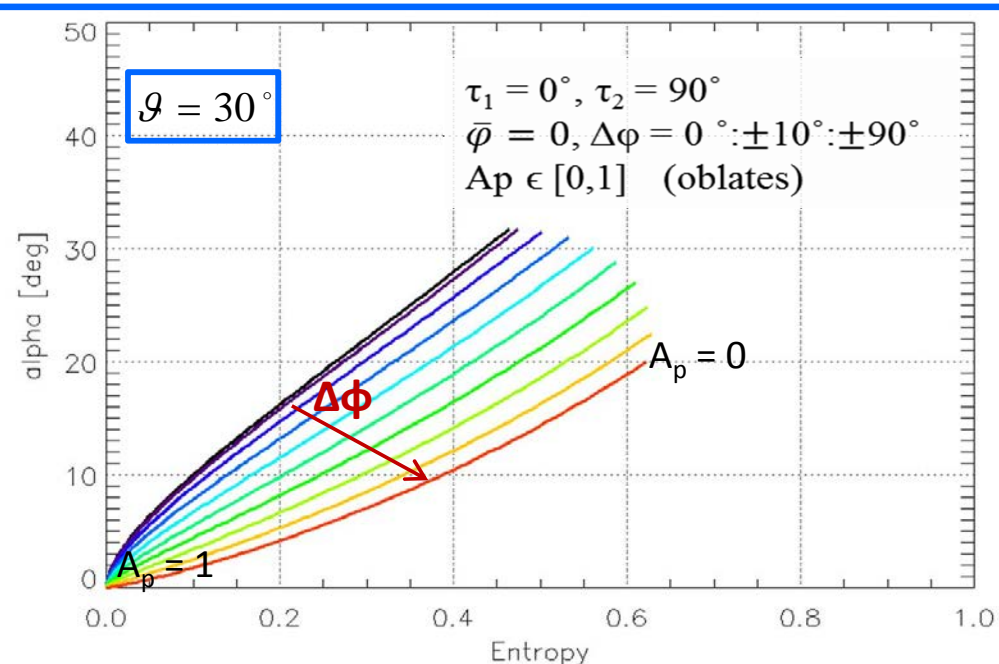
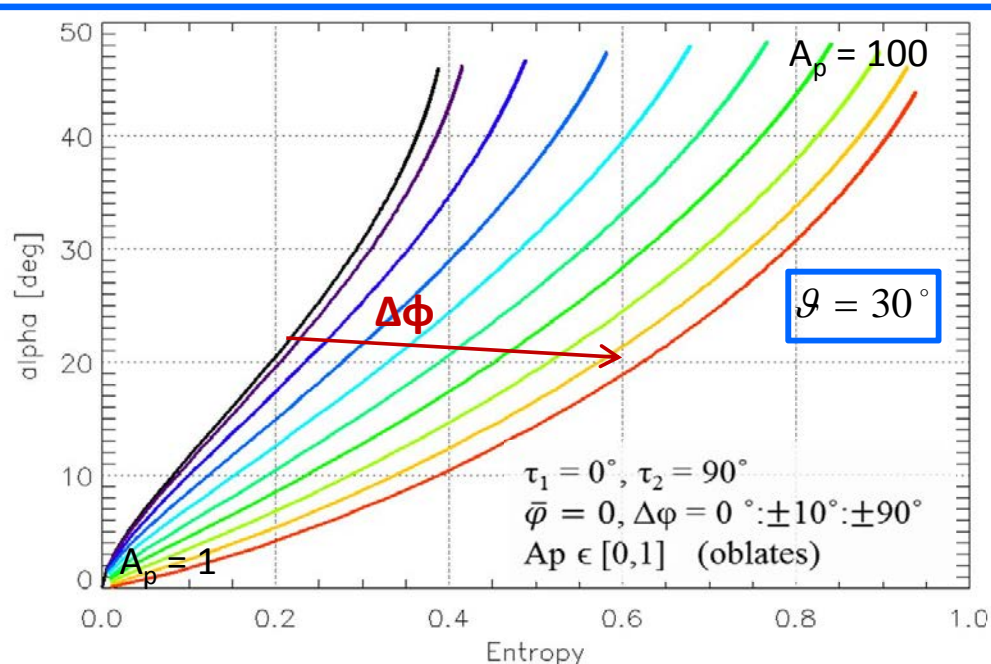
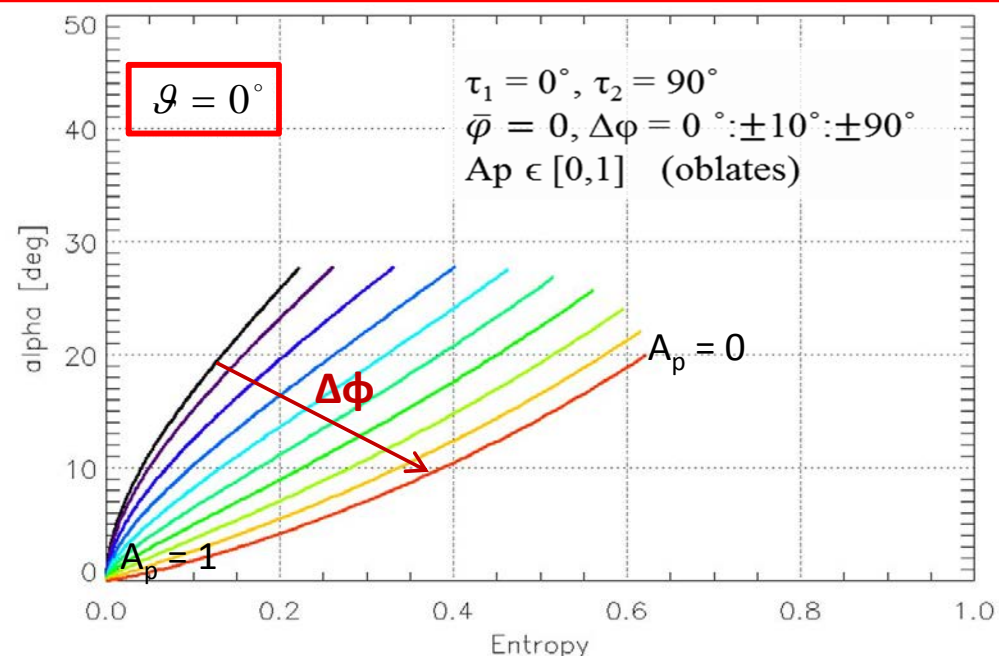
BACKUP

Scattering from a Cloud of Particles: AOI Dependency

Prolates



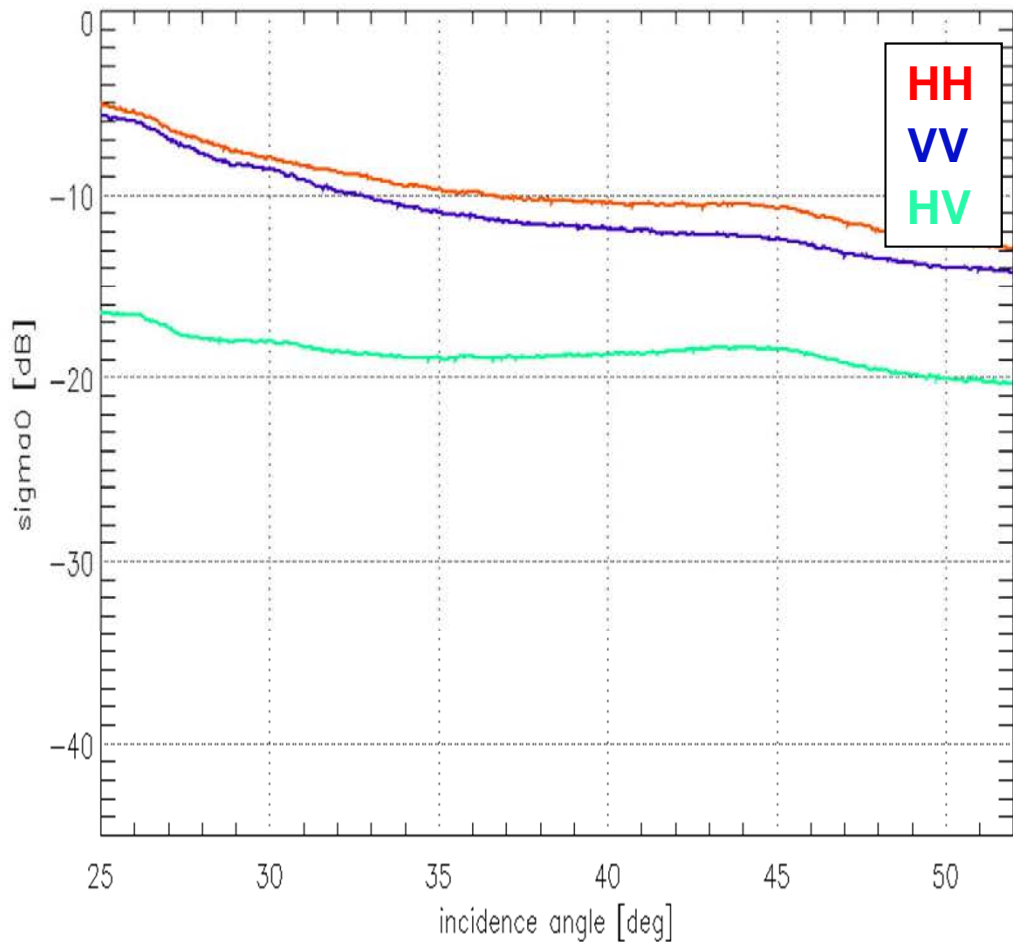
Oblates



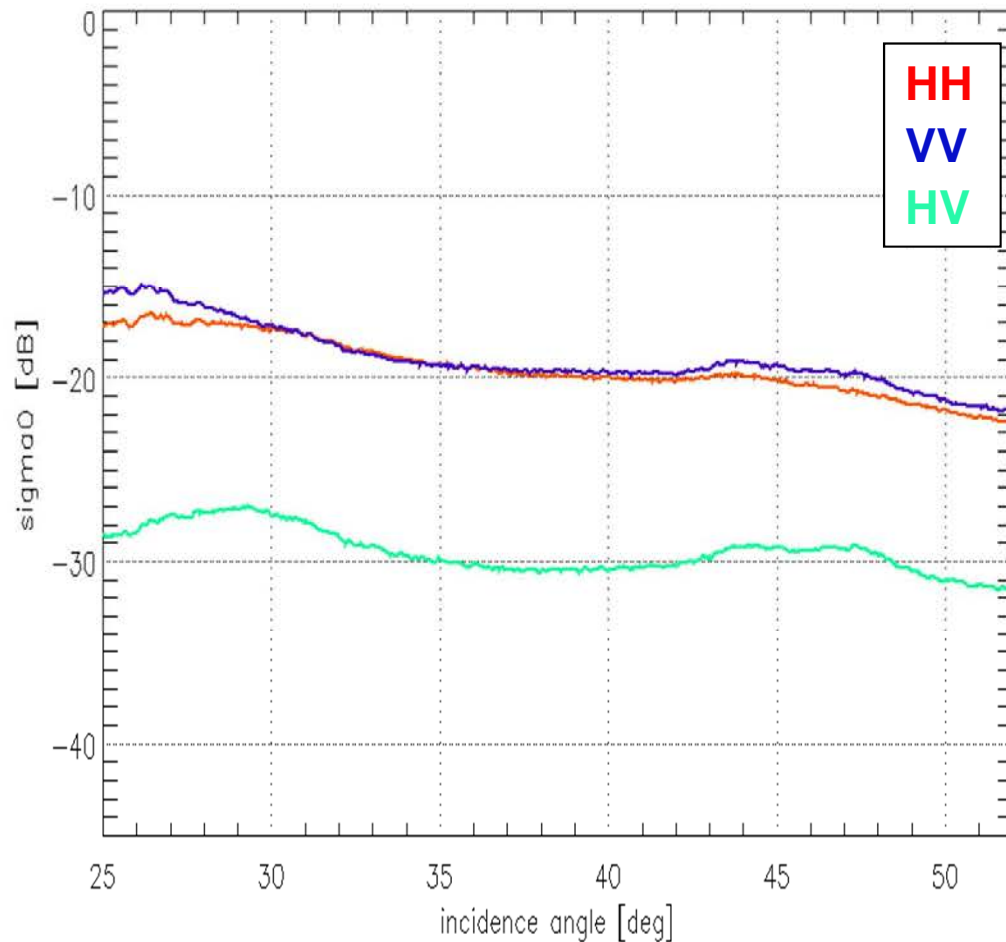
Summit, N, March

Backscattering vs AOI

L-band

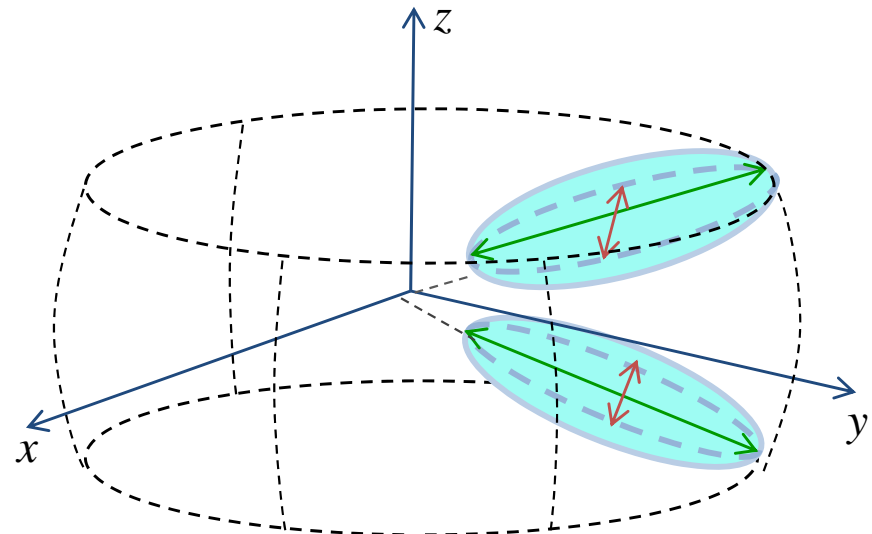


P-band

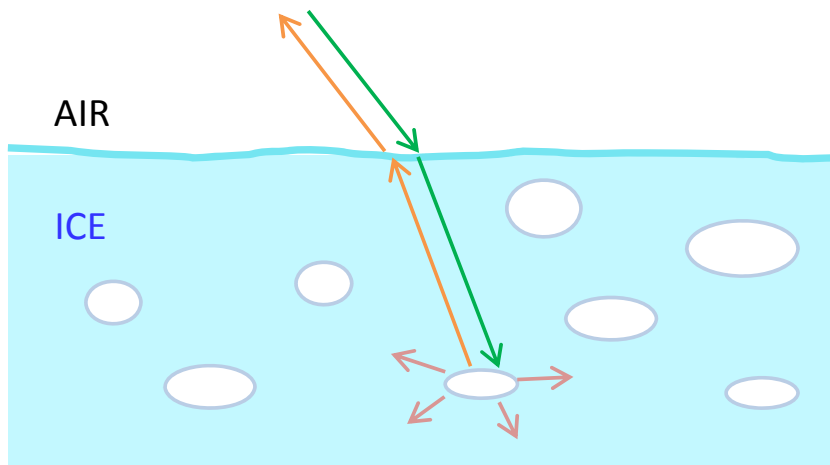


Simulated Scenario

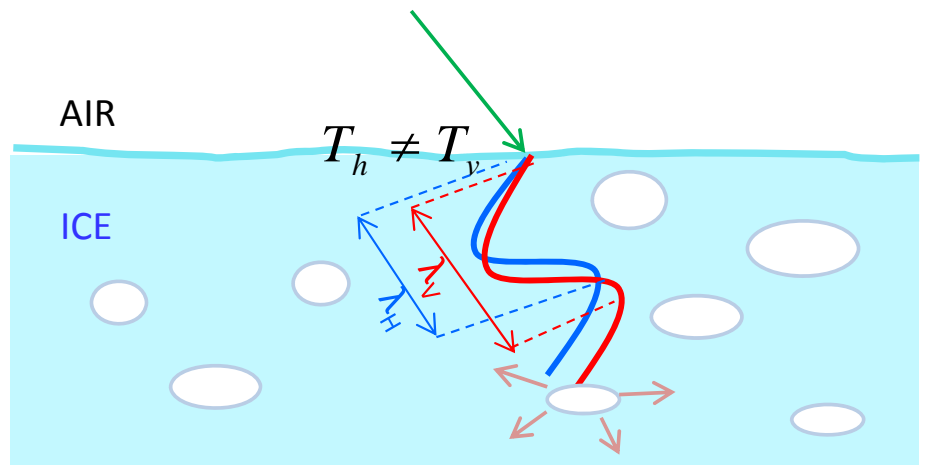
- ↗ **Horizontal oblate air bubbles**
- ↗ Limited tilt angle distribution (rotation around x-axis)
- ↗ Random canting angle (rotation around z-axis)
- ↗ **Penetration depth** of 15 m at L- and 35 m at P-band
- ↗ AOI from 25° to 50° (E-SAR)
- ↗ Simulated cases:



1) Particles cloud only

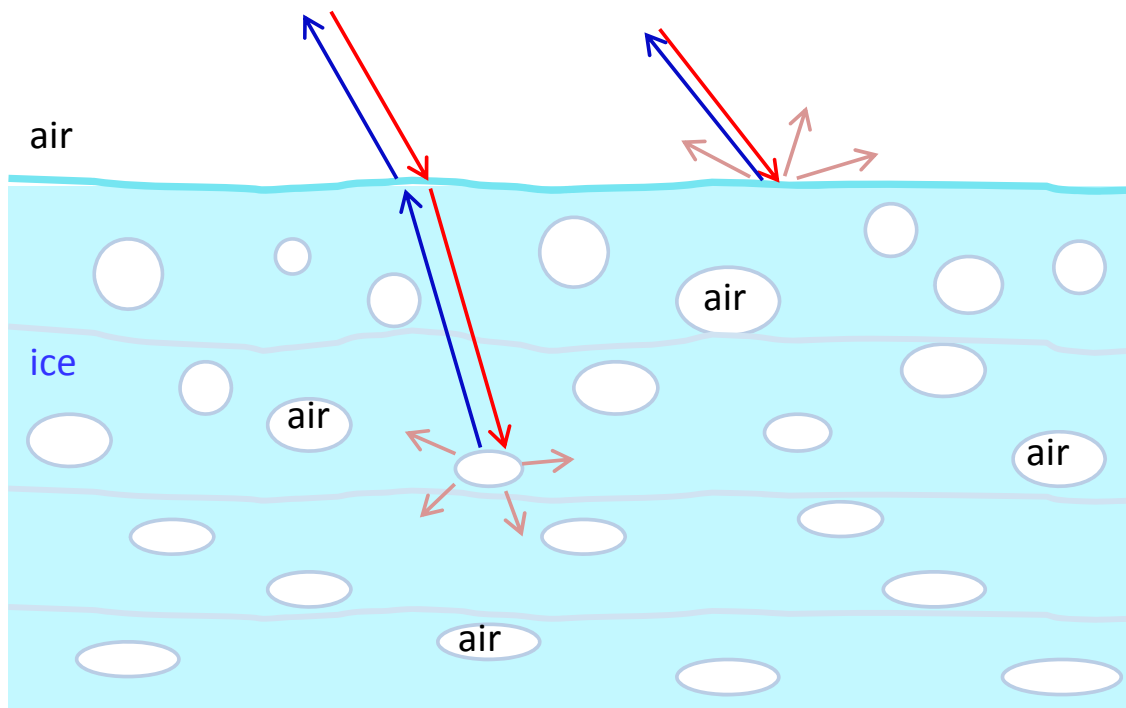


2) Particles cloud + transmission + differential propag. effects



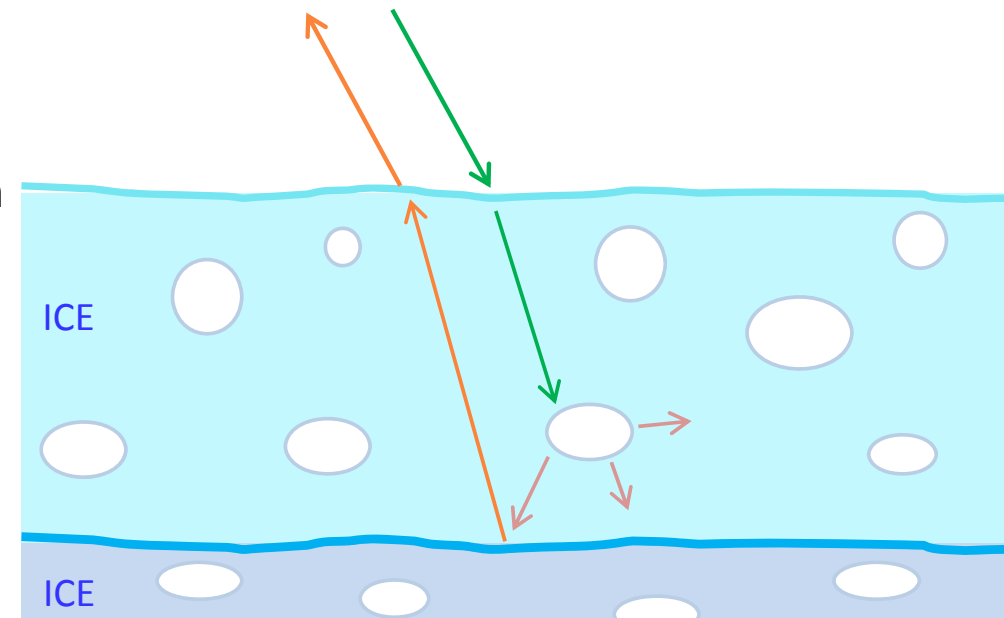
Air Bubbles in Glacier Ice

- ↗ **Air bubbles** get trapped when snow accumulates and becomes firn
- ↗ **Firn is richer** of bubbles than ice
- ↗ Bubbles occupy up to **10% of the ice volume** in the upper layers (several tens of m)
- ↗ Tendency to **disappear with depth** (bubble-free ice around 100-150m)
- ↗ Typical size range from **few mm to some cm**
- ↗ Generally are sphere-like, and **get flattened with depth/pressure**



Dihedral Component

- ↗ Scattering from **particles-subsurface** interaction
 - ↗ Firn-Ice interface
 - ↗ Presence of layered dielectric contrast
- ↗ **Weak component** compared to volume and surface
- ↗ Significant contribution to **copoliar phase**

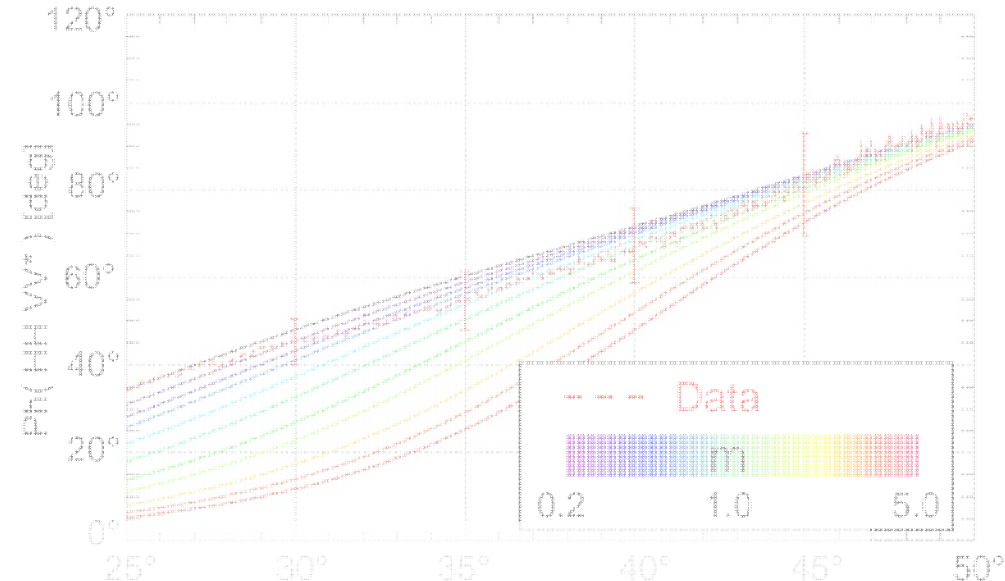
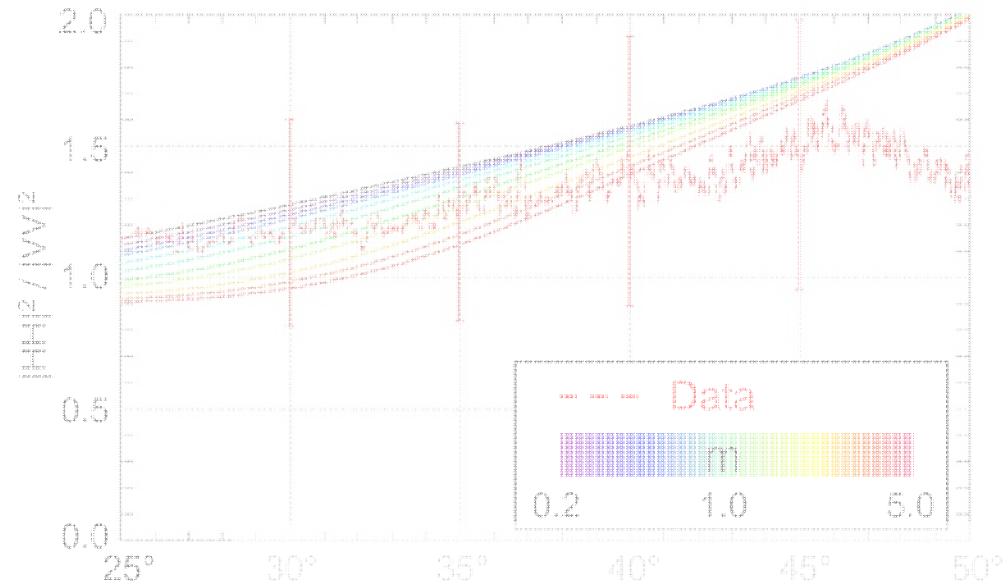


$$[C_{tot}] = f_s \cdot [C_{surf}] + f_v \cdot [T][P][C_{vol}][T]^t[P]^t + f_d \cdot [C_{dih}] + [N]$$

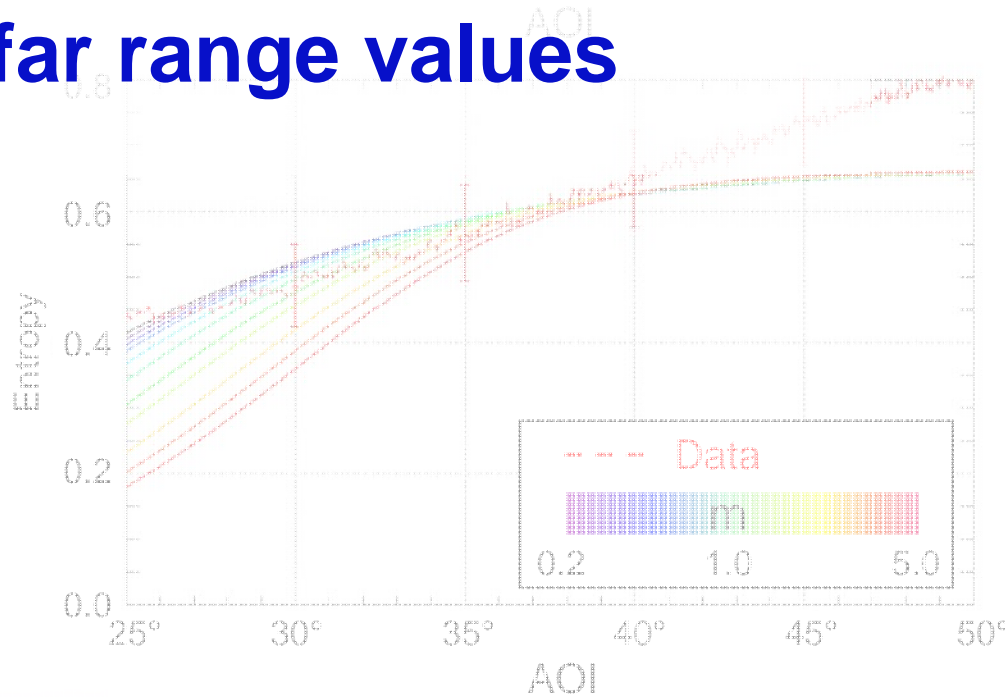
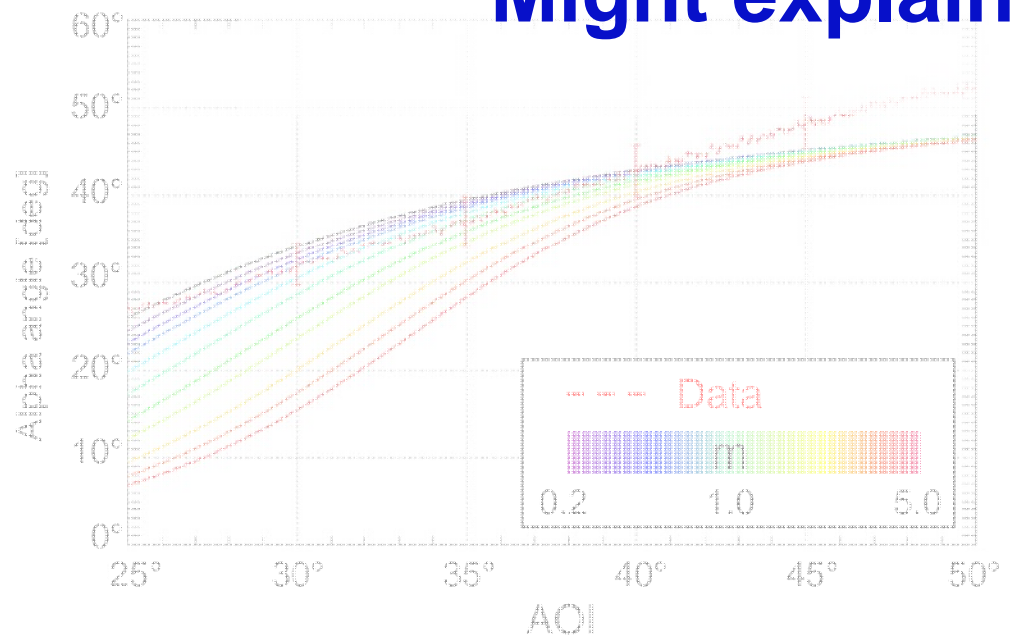
Outlook

- ↗ Include propagation and transmission effects

3 Components (Vol+Surf+Dihedral) vs L-band Data



Might explain far range values



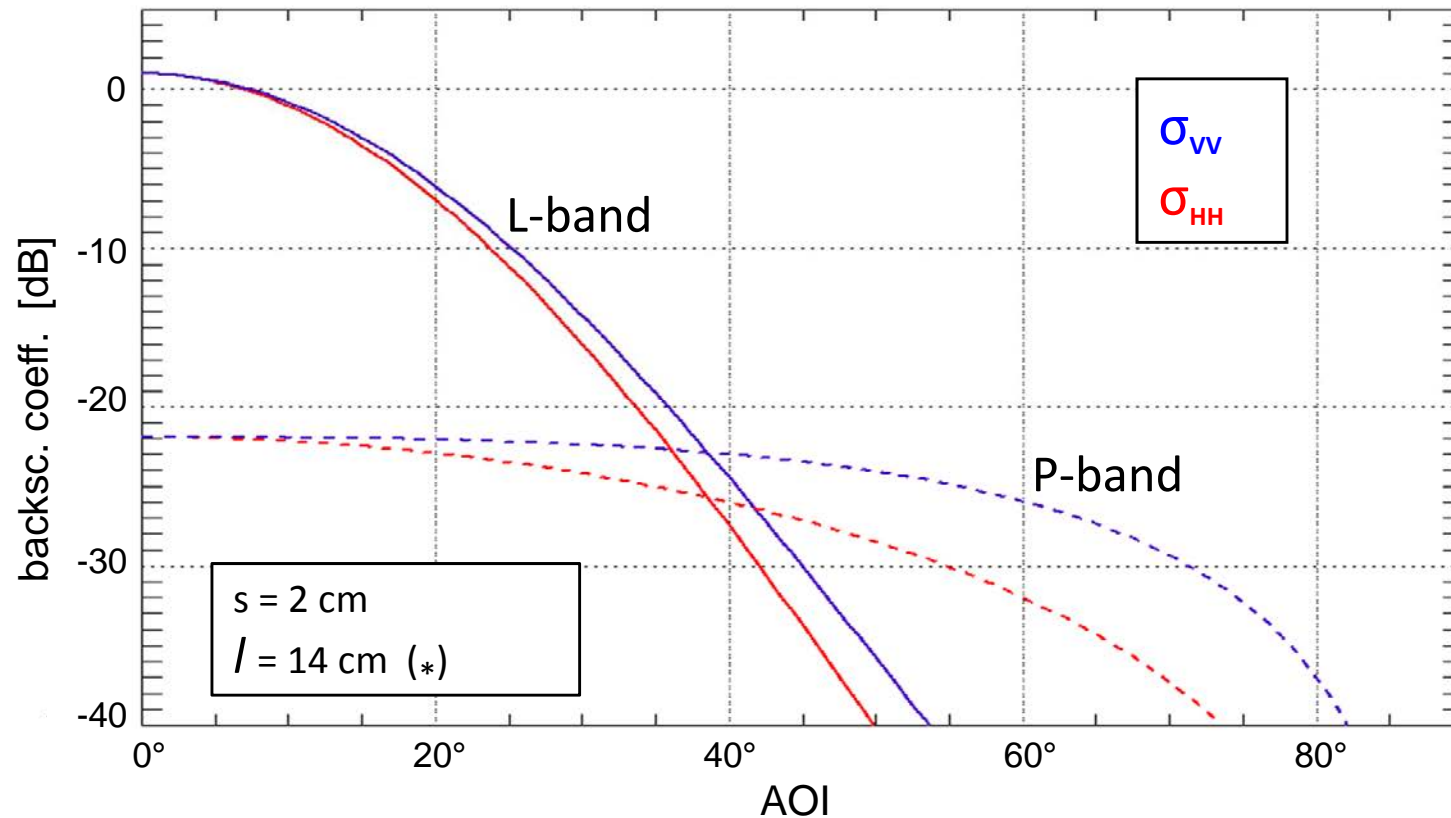
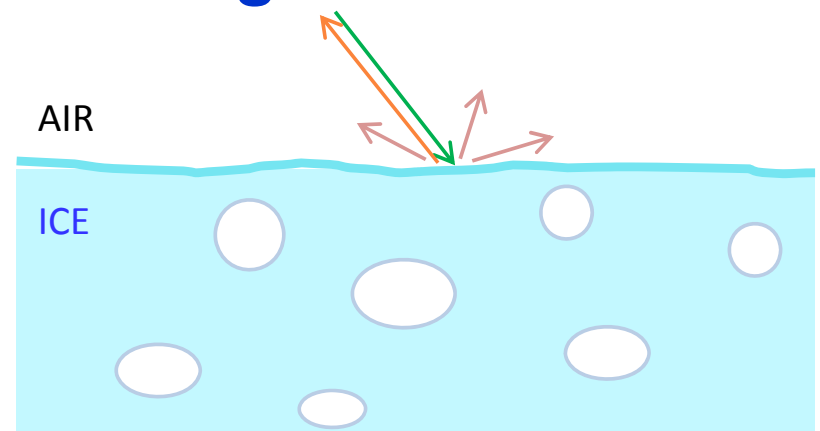
Modeling the Ice Surface – Bragg Scattering

Small Perturbations Model

s = standard deviation of vertical surface roughness

l = surface correlation length

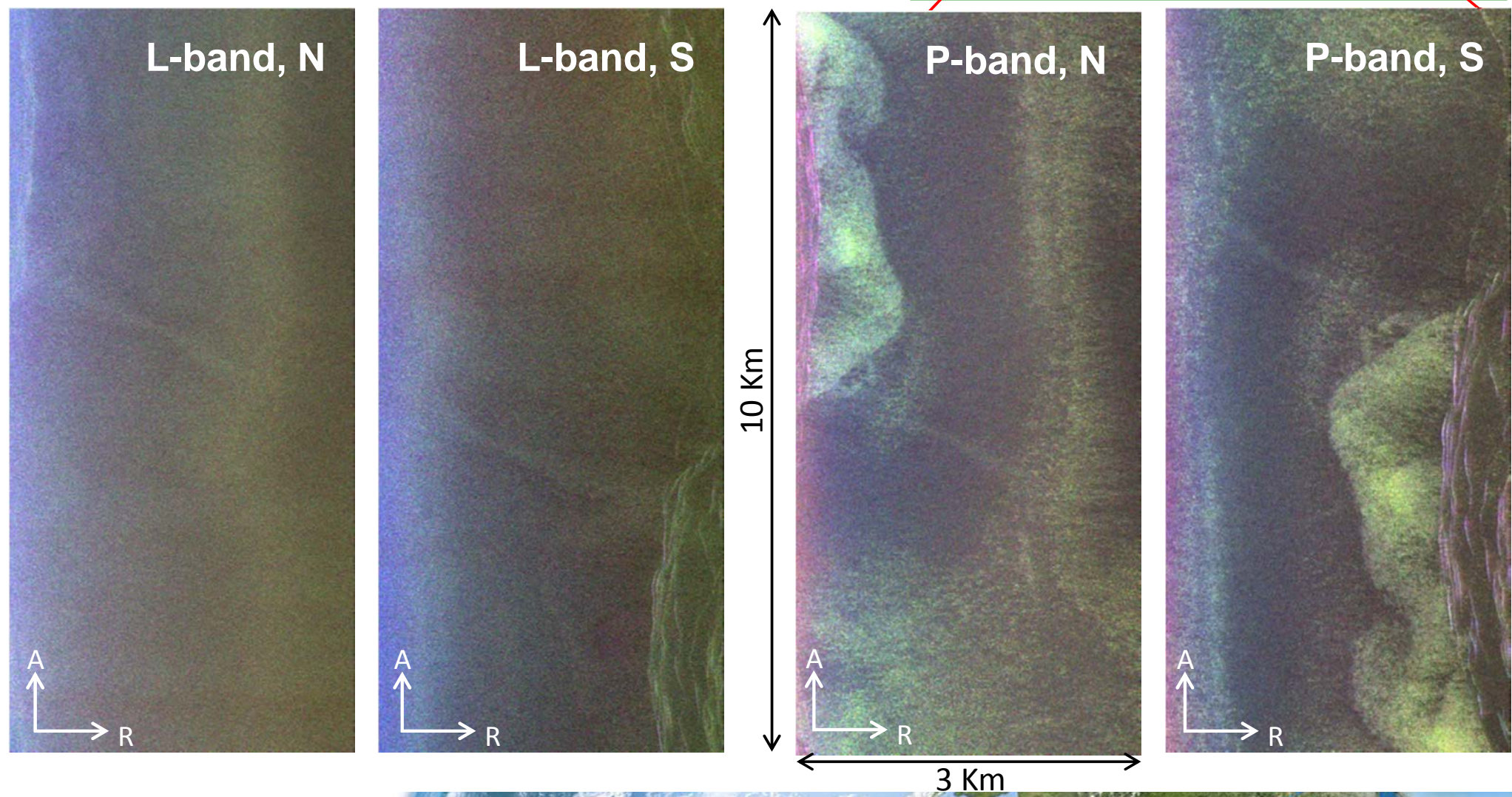
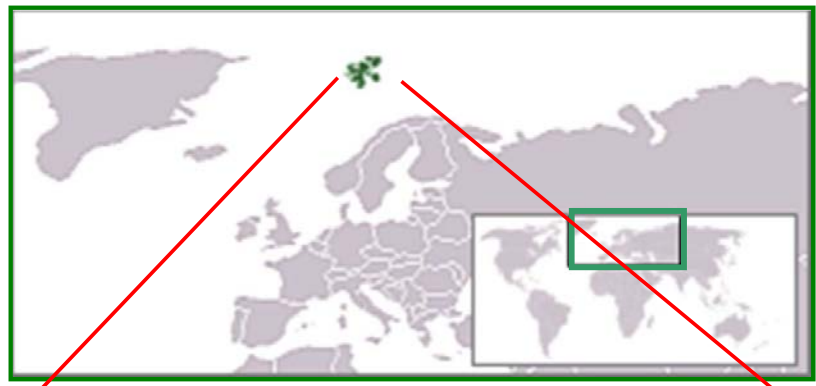
$$W_{surf}(l, \vartheta) = \frac{1}{2} l^2 e^{-(kl \sin \vartheta)^2} \text{ roughness spectrum}$$



(*) H. Rott, and R.E. Davis "Multifrequency and Polarization SAR Observation on Alpine Glaciers", *Annals of Glaciology*, vol.17, pp. 98-104, 1993.

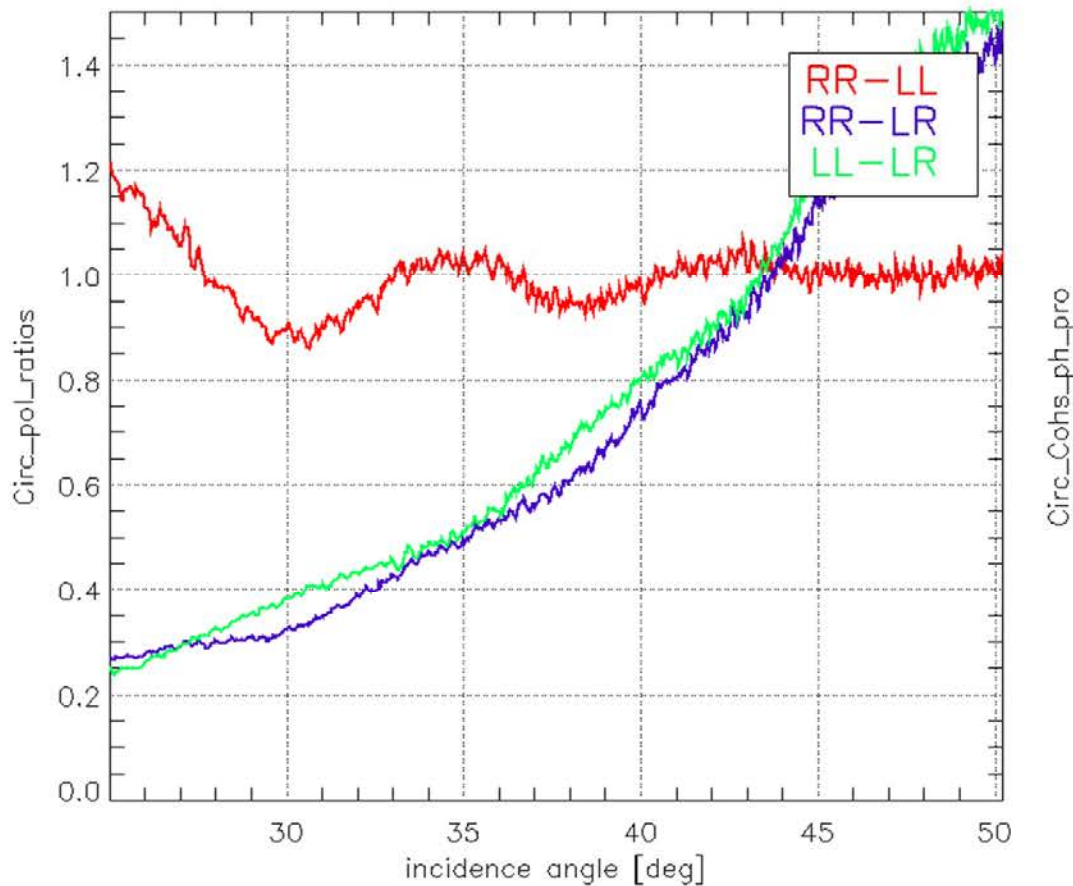
Test Site: Nordaustlandet, Svalbard

- **Summit of the Austfonna ice cap, Svalbard Archipelago, Norway ($\sim 80^\circ\text{N}, 24^\circ\text{E}$)**
- **Flat topography, max ice thickness $\sim 560\text{m}$**
- **IceSAR 2007** data, fully polarimetric, L- and P-band, South and North flights, **AOI** $25^\circ\text{-}50^\circ$

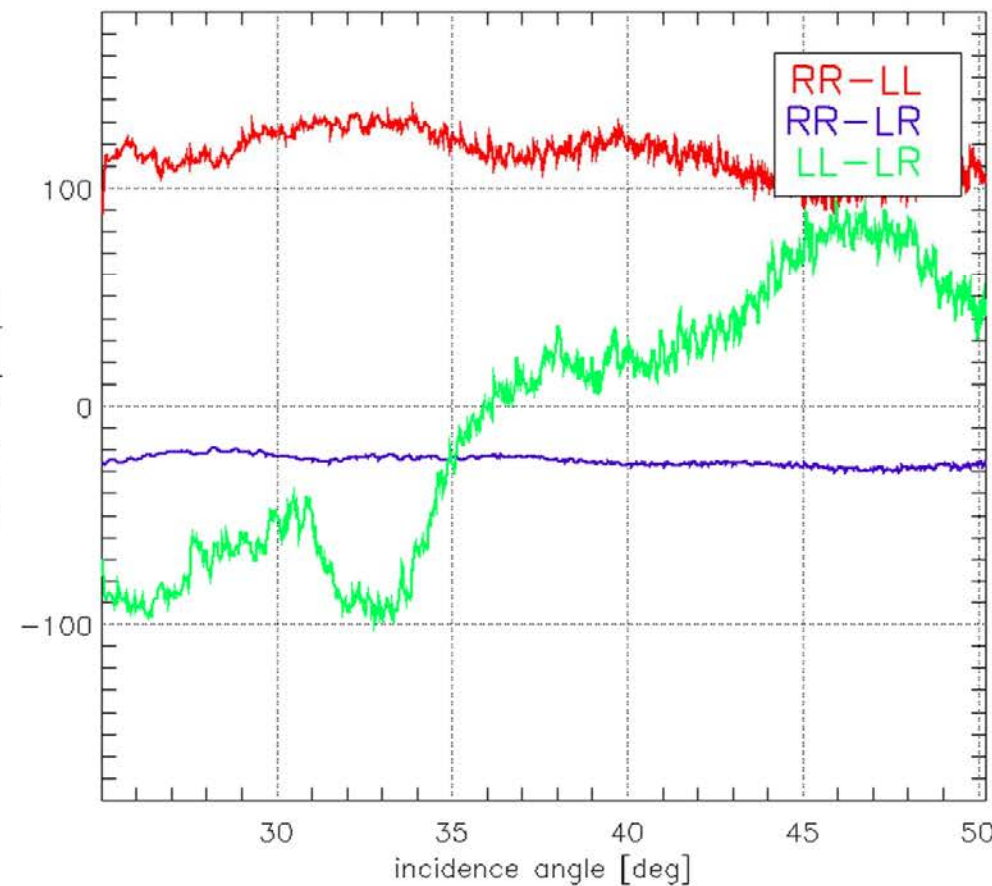


Summit, March, North, L-band – Circular Pol

Ratios

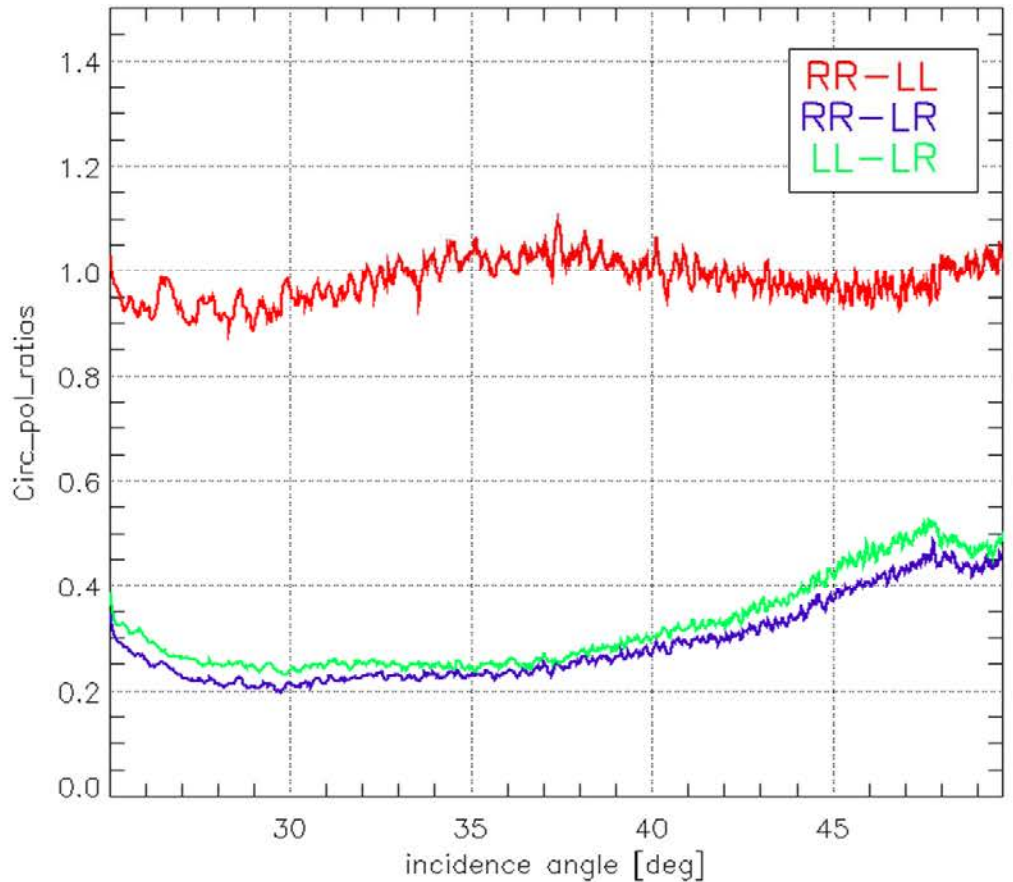


Phases

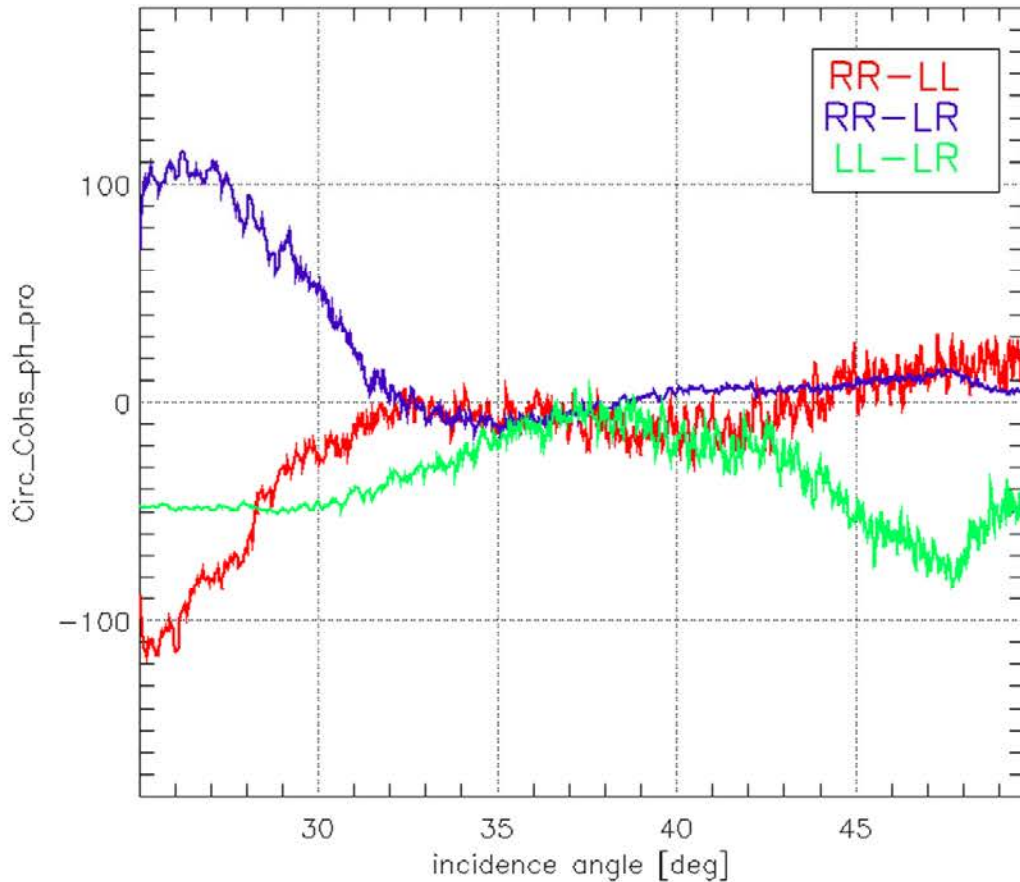


Summit, March, North, P-band – Circular Pol

Ratios

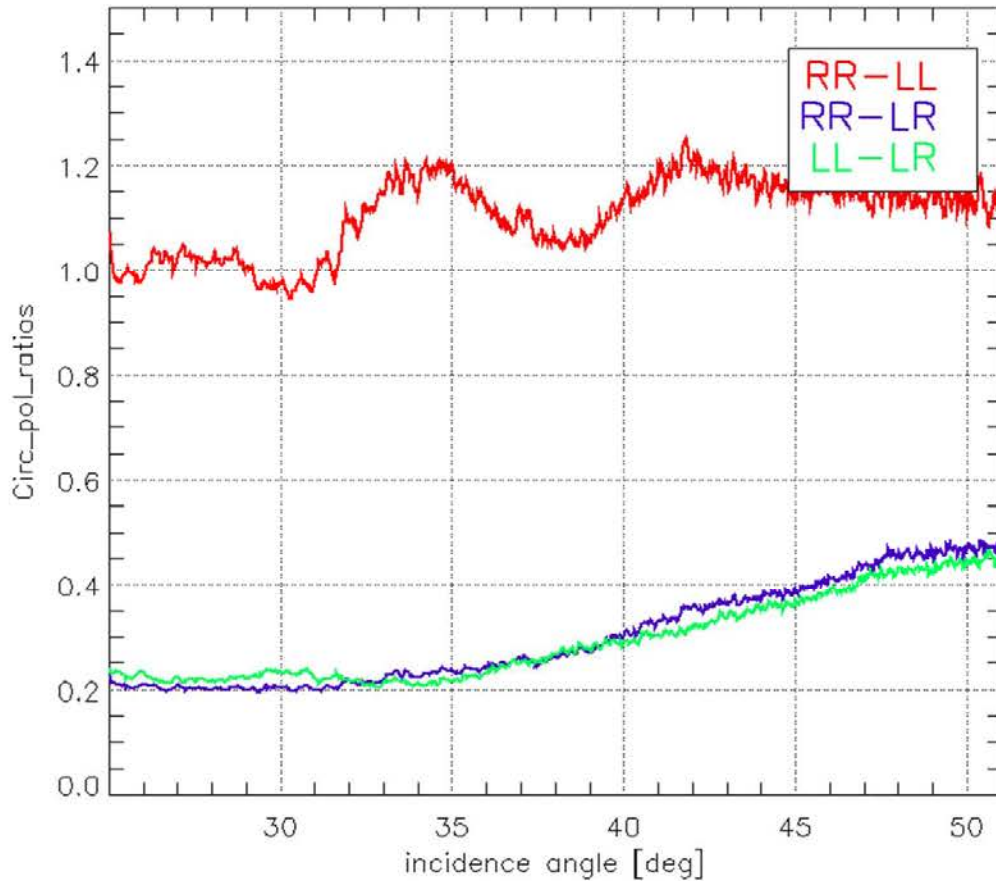


Phases

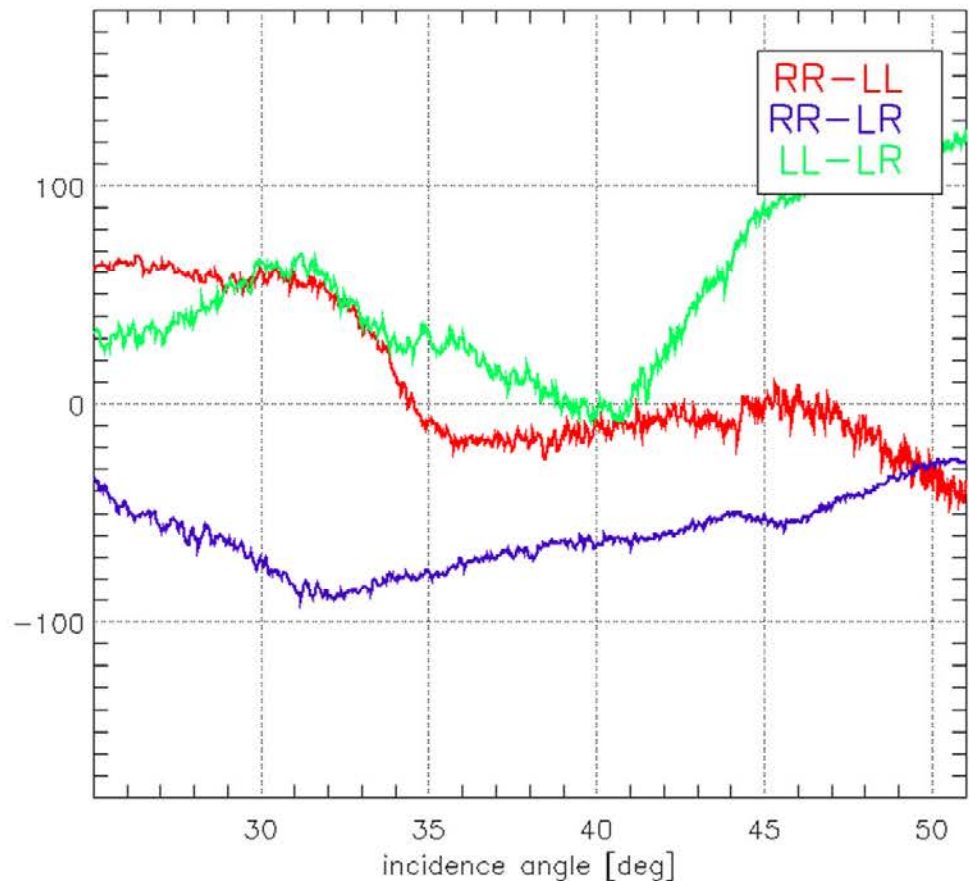


Eton, March, North, L-band – Circular Pol

Ratios

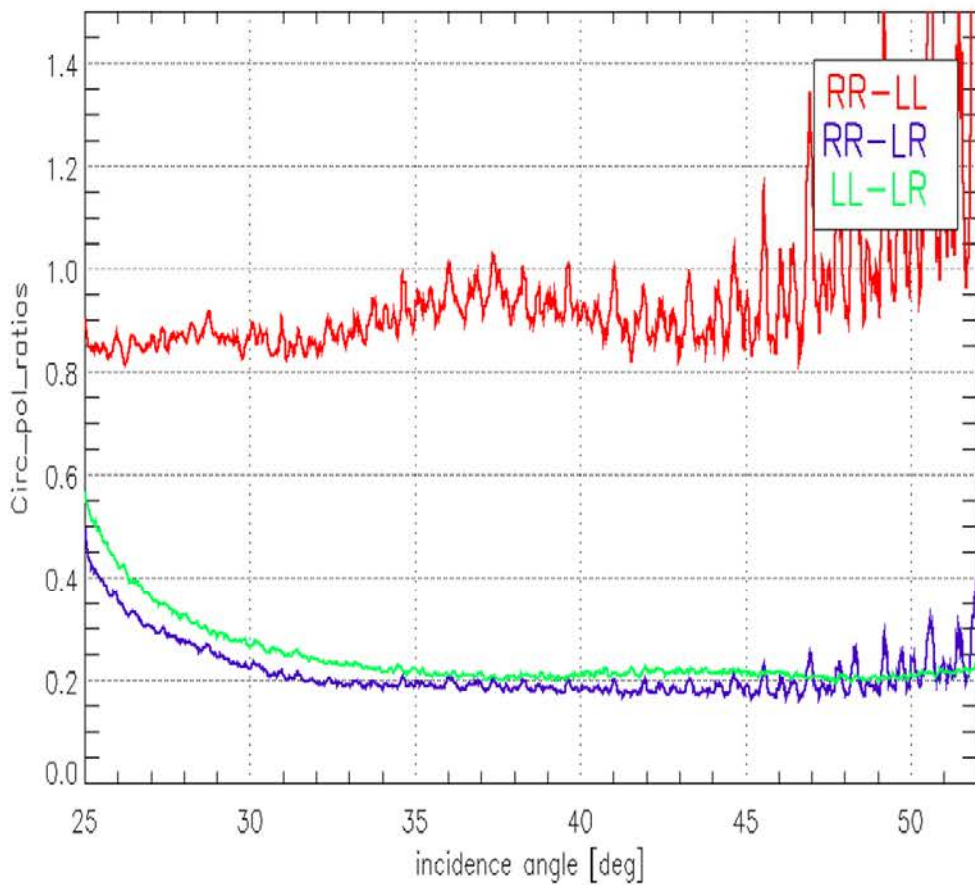


Phases

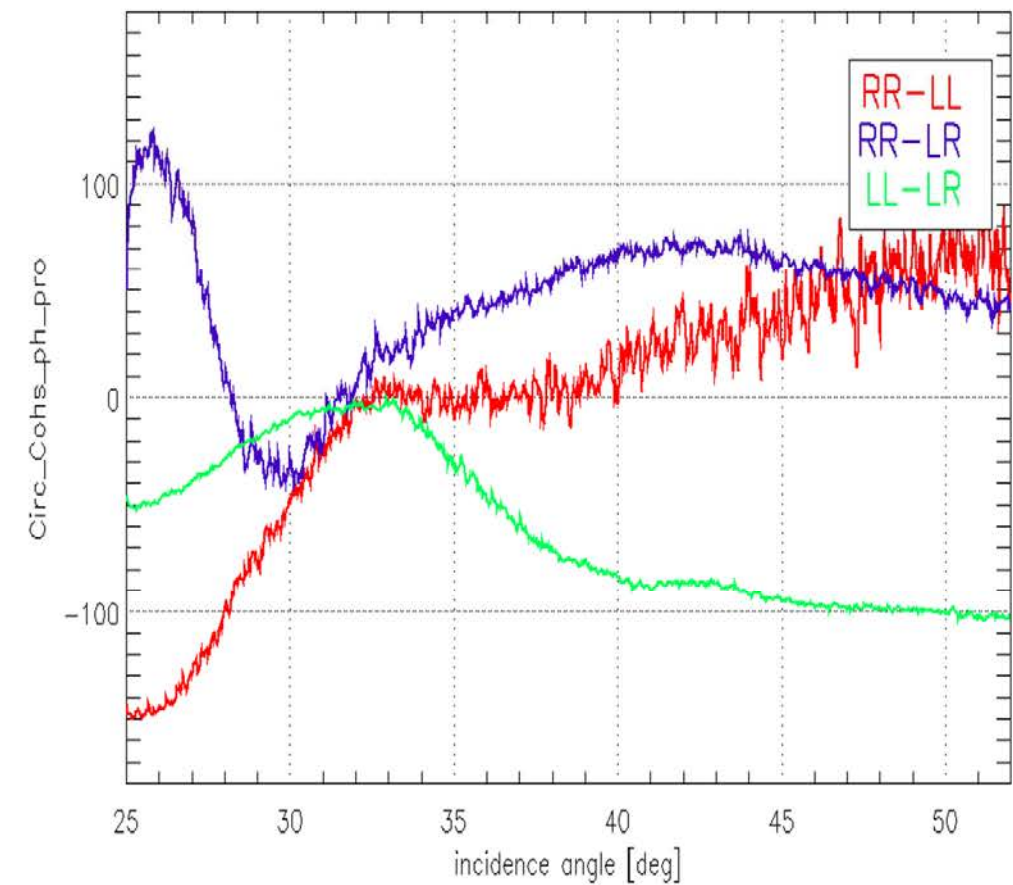


Eton, March, North, P-band – Circular Pol

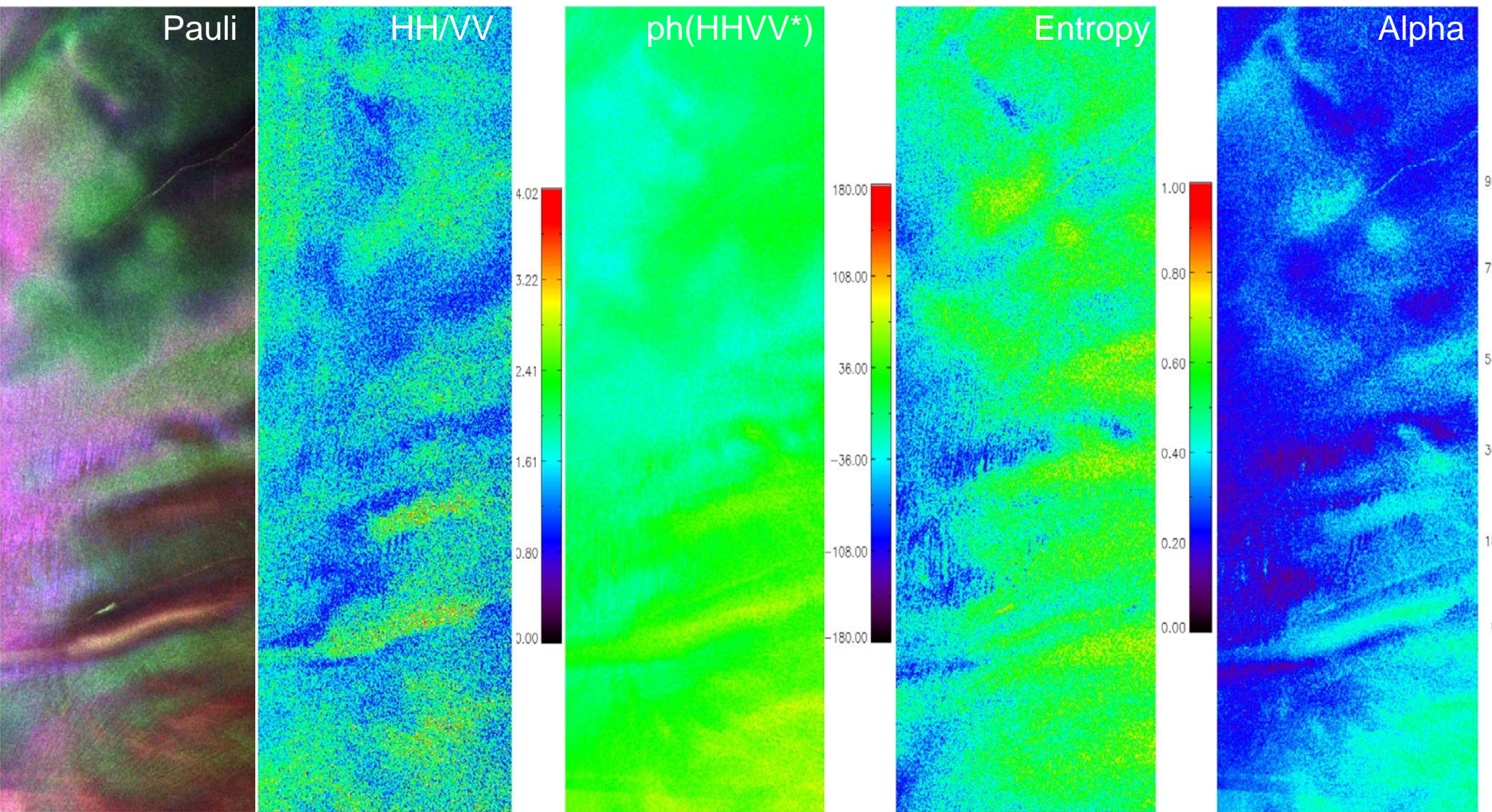
Ratios



Phases



Eton, N, April, L-band



Eton, N, April, P-band

